Tests of fundamental physical theories from measurements on free charged leptons

J. H. Field and E. Picasso

CERN, Geneva, Switzerland

F. Combley

Dept. of Physics, University of Sheffield, England
Usp. Fiz. Nauk **127**, 553–592 (April 1979)

After a brief introduction in which the concepts of the magnetic and electric dipole moments of particles are introduced and questions are discussed associated with the discrete P and T transformations, the main part of the paper follows which consists of two sections. In the first of these the validity of quantum electrodynamics is analyzed on the basis of measurements of the anomalous magnetic moments of electrons and muons. Special emphasis is placed on experimental methods of measurement and on their historical development. The most detailed description is provided of three recent experiments: 1) measurement of $(g-2)$ for muons at CERN; 2) the spin resonance experiment on single electrons at the University of Washington; 3) the precise comparison of electron and positron magnetic moments carried out using the VEPP-2M storage ring at Novosibirsk. In the next section a review is given of the tests of CPT, CP, and T invariance from muon decay correlations and lifetime measurements. Finally the present status of experimental searches for an electric dipole moment (the existence of which would violate both P and T invariance) of electrons and muons is discussed.

PACS numbers: 12.20.Fv, 13.10. + q, 11.30.Er, 14.60. – z

CONTENTS

1. INTRODUCTION

In this review we shall discuss measurements of the dipole moments of free electrons and muons, and of the lifetimes of free muons describing how these measurements have been used to test fundamental physical theories. When discussing these experiments we shall confine ourselves to considerations of physical principle rather than technical detail; fuller accounts of the experimental methods may be found in the original papers to which reference is made below, and also in several review articles.[1]

We note that a totally free particle is an idealized concept, and we use the term to mean particles so weakly bound that any shift in the value of the measured quantity due to this containment is negligibly small.

Classically the dipole moments can arise from either charges or currents. For example, the circulating current, due to an orbiting particle with an electric charge e and mass m, has associated with it a magnetic dipole moment μ_L given by

$$\mu_L = \frac{e}{2mc} \mathbf{L}, \tag{1.1}$$

where $\mathbf{L}$ is the orbital angular momentum. Alternatively, the electric dipole moment possessed by certain polar molecules is due to the relative displacement of the centers of the positive and negative

 0038-5670/79/040199-21$01.10

electric charge distributions. Thus we have examples of a magnetic dipole moment and an electric dipole moment both having their origins in electric charge, and it is of interest to note that all electromagnetic phenomena are explained in terms of electric charges and their currents; there is not place, as yet, for magnetic charges. In particular the intrinsic magnetic dipole moments of all particles can be considered, in the classical picture, to be made up of circulating electric currents and not of distributed magnetic charges.[2] This is just one aspect of the basic asymmetry between the electrical and magnetic parts of electromagnetism which is apparent from Maxwell's equations. The argument, first proposed by Dirac,[3] that the existence of magnetic charge leads naturally to the quantization of both magnetic and electric charges, still stands as a challenge to physicists, both theoretical and experimental, to find a proper place for the magnetic monopole in electromagnetic theory and establish its physical reality.

For a particle with both magnetic and electric dipole moments the electromagnetic interaction Hamiltonian contains a part

$$\mathcal{H} = -\mu_m \mathbf{B} - \mu_e \mathbf{E}, \tag{1.2}$$

where **B** and **E** are the magnetic and electric field strengths and μ_m and μ_e are the magnetic and electric dipole moment operators. Following the general form of Eq. (1.1) and treating the electric dipole moment analogously to the magnetic dipole moment, we write

$$\mu_m = g\frac{e}{2mc}\frac{\hbar\sigma}{2}, \quad \mu_e = f\frac{e}{2mc}\frac{\hbar\sigma}{2}, \tag{1.3}$$

where the components of σ are the three Pauli spin matrices and for the negative lepton we have to insert the charge $e = -|e|$. Making use of the Bohr magneton $\mu_0 = e\hbar/2mc$, these equations can be simplifed to

$$\mu_m = g\mu_0\frac{\sigma}{2}, \quad \mathbf{D} \equiv \mu_e = f\mu_0\frac{\sigma}{2}, \tag{1.4}$$

where we have taken the opportunity to introduce the conventional symbol for the electric dipole moment, D.

The main body of this paper is divided into two parts, the first of which contains an examination of the way in which the measurements of dipole moments have been used to test quantum electrodynamics (QED). This has been the principal motive for measurements of the lepton g-factor, introduced in the first of the equations (1.3). The interest has centered around the early realization that its value was not exactly equal to two as predicted by the Dirac theory.[4] We shall see, however, that in the broader context of QED, the observed electromagnetic interaction of both electrons and muons is in complete accord with the predictions of theory down to distances as small as 7×10^{-17} m.

In the second part we deal with tests of discrete symmetries using free leptons. We start with a discussion of the extent to which the validity of the CPT theorem has been checked by measurements on both particles and antiparticles. This is followed by an examination of the experimental evidence demonstrating invariance with respect to individual symmetry operations. Here we present the well-known argument that the expectation of the electric dipole moment D must be zero for a particle described by a state of well-defined parity. The polar molecules that we have referred to above are in a mixture of degenerate states with opposite parities and so are not covered by this symmetry condition. Arguments involving the time-reversal operation also require that the electric dipole moment should vanish. These requirements really stem from the different symmetry properties of the magnetic and electric fields. While **B** is an axial vector, **E** is a polar vector; thus if the Hamiltonian equation [Eq. (1.2) above] is to remain invariant with respect to parity inversion and time reversal, then μ_m must transform like an axial vector while μ_e must transform like a polar vector; an axial vector changes sign under T but not under P, while for a polar vector the opposite is true. Looking at equations (1.4), we see that the dipole moment operators should transform like the spin operator σ. Since this latter behaves like an axial vector, all is consistent for μ_m, but in the case of μ_e either of the operations P or T changes the relative sign of the two sides of the equation. The only way in which this situation can be satisfied is if f is zero. These arguments can be generalized to show that for a system of definite parity the odd electron (dipole, sextupole, etc.) and even magnetic (quadrupole, octupole, etc.) moments must be zero. Since the breakdown of parity, however, the invariance of interactions with respect to symmetry operations has always to be underpinned by experiment.

2. MEASUREMENT OF THE LEPTON g-FACTORS AS A TEST OF QED

In this section we shall only be concerned with the lepton magnetic dipole moment, since there is no place for an electric dipole moment of the electron or the muon within QED, the electromagnetic interaction being invariant with respect to parity inversion or time reversal.

Quantum electrodynamics can be considered as a clearly defined mathematical procedure whereby any process involving the interaction of the photon and charged lepton fields may be calculated to any order of approximation. It is not without its controversial points, however, and the existence of infinities within its structure remain difficult to accept, their presence precluding any real understanding of the fundamental constants such as charge and mass. The increasing order of the approximation involves the calculation of more and more successive interactions between the photon and lepton fields. All these terms depend upon the renormalization procedure in which the sum of the bare lepton mass and its (infinite) radiative correction is put equal to the observed rest mass of the particle, while the sum of the bare lepton charge and its (infinite) radiative correction is put equal to the observed electronic charge.

The target of experimentalists in this area has been twofold: on the one hand, to check the theory at smaller and smaller distances, looking for any evidence of the

structure of leptons or of some new interaction which may, for example, explain the difference in mass between the electron and the muon; and on the other hand to test the higher order corrections, including renormalization with measurements of the highest precision. The theory may also be limited by some ultimate granularity of space-time, but such a breakdown would have ramifications for all interactions.

For more than a quarter of a century, experiments of greater and greater precision, and theoretical calculations of increasing complexity, have been matched together in an extremely searching test of our understanding of the electromagnetic interaction. We will discuss measurements of the g-factor of both electrons and muons, but start off with a discussion of the theoretical predictions, including the contributions that the strong and weak interactions make to this dominantly electromagnetic property.

The outline of the theoretical framework is followed by an historical perspective, tracing the evolution of the experiments from early studies on atoms to the more recent ones on free leptons using the spin resonance and precession methods. The early history is related in more detail in the review articles of Kusch[5] and Crane;[6] and to a lesser extent in those listed under Ref. 1.

The section concludes with an examination of the most recent and precise experiments on the electron and muon and their results. These also serve as the most current examples of the spin resonance and precession techniques, respectively.

2.1 Theoretical predictions

The lepton g-factor may be expressed as a perturbation expansion of the form

$$g_l = 2\left[1 + \sum_n A_n^{(l)} \left(\frac{\alpha}{\pi}\right)^n + \sum_n B_n^{(l)} \left(\frac{\alpha}{\pi}\right)^n\right], \qquad l = e, \mu, \ldots, \tag{2.1}$$

where the part $g = 2$ just represents the result of the Dirac relativistic theory. The higher order terms involve an increasing number of interactions between photon and lepton fields and consequently take the form of a power series in the square of the coupling constant; that is, a series in the fine structure constant α. These higher order terms are here divided into two groups; those for which the coefficients are independent of lepton mass A, being separated from those for which the coefficients are a function of the ratio of the mass of the external lepton to that of the lepton in the vacuum polarization loops. The first sequence of terms is the same for any lepton, while the second, which commences with $n = 2$, is only significant in the case of the muon and heavier leptons owing to the fact that the muon mass is some 200 times bigger than that of the electron. These two sequences constitute the so-called anomaly a defined by

$$a_l \equiv \frac{g-2}{2} = \sum_n A_n^{(l)} \left(\frac{\alpha}{\pi}\right)^n + \sum_n B_n^{(l)} \left(\frac{\alpha}{\pi}\right)^n. \tag{2.2}$$

The coefficient of the leading term was first shown by Schwinger[7] to be $A_1^{(l)} = 0.5$, from which it can be seen that the order of magnitude of the anomaly is 10^{-3}.

TABLE 2.1. Coefficients of the perturbation series in (α/π) for a_l up to $(\alpha/\pi)^4$.

n	$A_n^{(l)}$	$B_n^{(\mu)}$	$A_n^{(l)}(\alpha/\pi)^n \cdot 10^9$	$B_n^{(\mu)}(\alpha/\pi)^n \cdot 10^9$
1	0.5	0	1 161 409.8±0.3	0
2	−0.32848	1.09426	−1772.3	5904.1
3	1.188±0.017	23.26±0.05	14.9±0.2	291.5±0.6
4	?	128±70	?	3.7±2.1

When advantage was taken of this fact in the evolution of experimental techniques, and a way found to measure the anomaly directly rather than the g-factor itself, there was a considerable jump forward in the precision with which g was determined.

In Table 2.1 we list the values of the perturbation expansion coefficients together with the complete contribution to the anomaly. As noted above, $B_n^{(e)}$ is negligibly small.

The numerical values in the last two columns have been obtained using $\alpha^{-1} = 137.035\,987(29)$ as given by Olsen and Williams[8] after combining their new measurement of the proton gyromagnetic ratio at low field with the value of e/h obtained from the a.c. Josephson effect.[9]

In Fig. 1 the Feynman graphs associated with the coefficients $A_1^{(l)}$, $A_2^{(l)}$, and $B_2^{(\mu)}$ are shown. The difference between the graph for $B_2^{(\mu)}$ and the first one contributing to $A_2^{(\mu)}$ lies in the fact that while for $A_2^{(l)}$ the external lepton is of the same type as that in the vacuum polarization bubble, for $B_2^{(\mu)}$ this is not the case. The various parts which make up this latter coefficient have been calculated by Suura and Wickmann[10]; Peterman[11]; Elend[12]; and Erickson and Liu.[13] The seven diagrams which contribute to $A_2^{(l)}$ were determined analytically by Karplus and Kroll[14] and later recalculated and corrected by Peterman[15] and Sommerfield.[16]

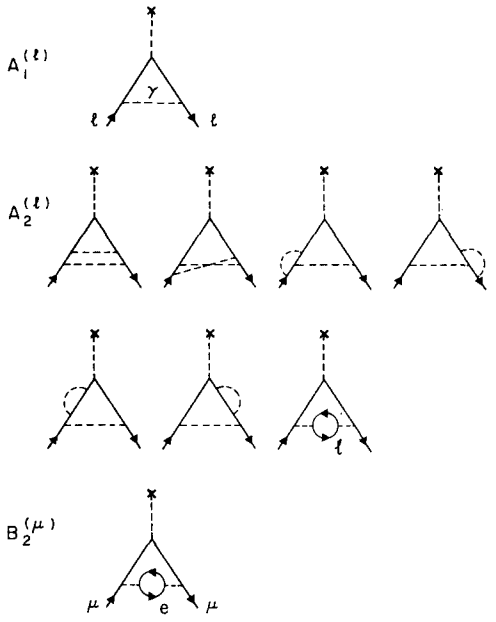

FIG. 1. Feynman graphs contributing to the QED part of the lepton anomalous magnetic moment up to order α^2.

For $A_3^{(I)}$ we have used the value given by Levine, Perisho and Roskies.[17] These authors combined their analytical results with those of Levine and Roskies[18]; Barbieri, Caffo and Remiddi[19]; Mignaco and Remiddi[20]; Barbieri and Remiddi[21]; and the numerical calculations of Cvitanovic and Kinoshita[22]; Calmet and Peterman[23]; Aldins, Brodsky, Dufner and Kinoshita[24]; and Chang and Levine.[25] More recently, three more of the contributing graphs have been evaluated analytically by Levine and Roskies.[26] It is a remarkable achievement on the part of these authors that between them they have calculated all 72 Feynman graphs which contribute to this coefficient.

The value quoted for $B_3^{(\mu)}$ contains the result of the numerical calculation of the six so-called light-by-light scattering graphs by Samuel and Chlouber,[27] which is slightly higher than the less precise but pioneering calculation of Aldins, Brodsky, Dufner and Kinoshita[24] and the more recent one of Calmet and Peterman.[28] Even more recently the analytical calculation of Lautrup and Samuel[29] has produced a value very close to that quoted here. The value of $B_3^{(\mu)}$ also contains the analytical results for the remaining set of 18 graphs obtained by Barbieri and Remiddi.[30] These results are in good agreement with the earlier calculation of various individual contributions to the set by Kinoshita[31]; Lautrap and de Rafael[32]; Lautrup[33]; Lautrup, Peterman and de Rafael[34]; and Brodsky and Kinoshita.[35]

The value for $B_4^{(\mu)}$ quoted in the table is taken from the work of Calmet, Narison, Perrottet and de Rafael,[36] who also review all the theoretical contributions to the anomalous magnetic moment of the muon. This recent work on the eighth-order QED contribution is consistent with the earlier estimates of Lautrup[37] and Samuel.[38]

Putting the numerical results together and recalling that the B coefficients for the electron are negligible, we obtain the predicted values for the anomaly according to QED:

$$a_e^{\mathrm{QED}} = (1\,159\,652.4 \pm 0.4)\cdot 10^{-9},$$
$$a_\mu^{\mathrm{QED}} = (1\,165\,851.7 \pm 2.3)\cdot 10^{-9}, \qquad (2.3)$$

where the errors are the quadratic sum of those due to the uncertainty in α^{-1} and those arising from the numerical calculations.

Thus the determination of the anomaly within QED can in principle be carried through with limitless precision, as more and more terms are reduced to an analytical form. However, it should be noted that at each order the number of graphs increases considerably; for example, although there is only one contributing to $B_2^{(\mu)}$, there are 24 diagrams associated with $B_3^{(\mu)}$, and for $B_4^{(\mu)}$, even if those which vanish as $m_e/m_\mu \to 0$ are eliminated, there remain 469. Thus in practice the rapidly increasing complexity of the calculations forms a barrier to indefinite improvements in precision. It must also be remembered that comparison between theory and experiment will always depend upon the separate determination of the fine structure constant α.

Before we can proceed to such comparisons, however, we have to examine the contributions to the anomaly which come from the strong and weak interactions. The former enter through the vacuum polarization into hadronic states. The lepton is coupled to these states by the virtual photon; thus the process bears a resemblance to electron-positron annihilation into hadrons. This link is exploited by means of dispersion relations. Under the assumption that the annihilation is dominated by the single photon process, we may write this hadronic contribution to the anomaly as

$$a_{(\mathrm{hadronic})} = \frac{1}{4\pi^3}\int_{4m_\pi^2}^{\infty} ds\,\sigma_{e^+e^-\to\mathrm{hadrons}}(s)\,K(s), \qquad (2.4)$$

where s is the total e^+e^- center-of-mass energy squared. The function $K(s)$ is a purely QED quantity arising from the combination of the two lepton propagators and the propagator of a virtual photon with mass $\sqrt{s}$ at the lepton vertex:

$$K(s) = \int_0^1 dx\,\frac{x^2(1-x)}{x^2+(1-x)(s/m^2)}, \qquad (2.5)$$

with m the lepton mass. In the region of integration of Eq. (2.4) the function $K(s)$ is positive definite and in the limit $s \gg m^2$ it has the value $\frac{1}{3}m^2/s$. With the additional assumption of electron-muon universality, these formula can be applied to the muon anomaly, and in fact the asymptotic dependence of the function $K(s)$ on the square of the lepton mass indicates that the hadronic contribution to the muon moment will be some 10^5 times larger than the hadronic part of the electron moment. This means that the electron moment is essentially a pure QED quantity.

The most recent determinations of the contribution to the muon anomaly are those of Barger, Long and Olsson[39]:

$$a_{\mu\,(\mathrm{hadronic})} = (66 \pm 10)\cdot 10^{-9}, \qquad (2.6)$$

and of Calmet, Narison, Perrottet and de Rafael,[40]

$$a_{\mu(\mathrm{hadronic})} = (66.7 \pm 9.4)\cdot 10^{-9}. \qquad (2.7)$$

These latter authors have included an estimate of higher order $[(\alpha/\pi)^3]$ hadronic effects which they find to be negative and at the level of 5% of the over-all hadronic contribution. The latest estimates quoted here replace the earlier ones of Gourdin and de Rafael[41] and Bramon, Etim and Greco.[42]

The contribution to the muon anomaly due to weak interactions can be calculated unambiguously within the framework of the renormalizable spontaneously broken gauge theories. These calculations have been carried out for different models by Jackiw and Weinberg[43]; Bardeen, Gastmans and Lautrap[44]; Bars and Yoshimura[45]; Fujikawa, Lee and Sanda[46]; Primack and Quinn[47]; and Discus.[48] More recently, the weak contribution to the anomaly is an arbitrary gauge model has been given by Leveille.[49] The results vary slightly are covered by the approximate relationship

$$a_{\mu\,(\mathrm{weak})} \approx 2\cdot 10^{-9}. \qquad (2.8)$$

Before the advent of the gauge theories, estimates given by Brodsky and Sullivan[50] and Burnett and Levine[51] had been an order of magnitude larger and of the oppo-

site sign.

The weak interaction contribution to the electron anomaly is much smaller, being at the level of less than 10^{-13}. The theoretically predicted value of the electron anomaly is thus just that given for QED [Eq. (2.3)], while the muon anomaly has to include these strong and weak interaction effects. The final values are

$$\begin{aligned} a_e &= (1159652.4 \pm 0.4)\cdot 10^{-9}, \\ a_\mu &= (1165920 \pm 10)\cdot 10^{-9}, \end{aligned} \tag{2.9}$$

where we have used $a_\mu(\text{weak}) = (2 \pm 2)\times 10^{-9}$ and the value of a_μ (hadronic) quoted in Eq. (2.7).

This brief summary in no way does justice to the immense amount of work carried out by many physicists over the last 30 years or so. The true dimension of this achievement can only be appreciated by studying the original papers. We have attempted to cover the most recent references, and a full discussion of the earlier work is given in the review of Lautrup, Peterman and de Rafael.[52]

2.2 Historical perspective and experimental principles

As indicated above, Dirac[4] had shown in 1928 that a value of 2 for the electron g-factor followed from his relativistic equation. Evidence that this was not in exact agreement with experiment can be seen, in retrospect, from early measurements of the hyperfine levels in hydrogen,[53] although at the time these were thought to have their origins in nuclear size effects. It was not until the discrepancy was more clearly defined by the precise experiments of Nafe, Nelson and Rabi[54] on the hyperfine structure separation in both hydrogen and deuterium, that Breit[55] put forward an explanation in terms of an anomalous part to the electron magnetic dipole moment. This anomalous part increases the over-all value to slightly larger than one Bohr magneton.

After the suggestion of Breit, the electron g-factor was extracted from atomic beam magnetic resonance measurements carried out on several different atoms by Kusch and Foley.[56] For each atomic state the value of g_J was obtained from measurements of the transition frequencies between the Zeeman levels of the hyperfine structure. For Russell-Saunders coupling, $g_J + \alpha_L g_L + \alpha_S g_S$ with

$$\begin{aligned} \alpha_S &= \frac{J(J+1)+S(S+1)-L(L+1)}{2J(J+1)}, \\ \alpha_L &= \frac{J(J+1)+L(L+1)-S(S+1)}{2J(J+1)}. \end{aligned} \tag{2.10}$$

Assuming that g_J is entirely due to a single electron and writing $g_L = 1$; $g_S = 2(1 + a_e)$, then

$$g_J = (\alpha_L + 2\alpha_S) + a_e(2\alpha_S). \tag{2.11}$$

Uncertainties associated with the value of the magnetic field were removed by taking ratios of the frequencies corresponding to the Zeeman splitting of different states. An example of the results obtained by these authors are those for gallium in which the ratio of g_J was determined for the $^2P_{1/2}$ ground state ($\alpha_S = -\frac{1}{3}$; $\alpha_L = \frac{4}{3}$) and the $^2P_{3/2}$ metastable state ($\alpha_S = \frac{1}{3}$; $\alpha_L = \frac{2}{3}$). In this case

$$\frac{g_{3/2}}{g_{1/2}} = \frac{2+a_e}{1-a_e} \approx 2 + 3a_e, \tag{2.12}$$

where the approximation is taken to first order in the anomaly a_e. From experiments on gallium, sodium, and indium, Kusch and Foley[57] were able to conclude that:

$$a_e = (1.19 \pm 0.05)\cdot 10^{-3}, \tag{2.13}$$

or

$$g = 2\,(1.00119 \pm 0.00005),$$

where the g without a subscript refers to the free electron g-factor. These measurements established the anomalous part of g, although there remained doubts in the form of relativistic corrections, and the interaction of the valence electron with the other electrons in the atom. It was plausibly argued that these corrections were within the experimental error, but their presence underlined the fact that improvements in the precision with which the anomaly was measured would ultimately require experiments on free particles.

The next development in the determination of the anomaly involved the combination of the results of two experiments. In 1949 Gardner and Purcell[58] had measured the resonance frequency of the proton and the cyclotron frequency of the free electron in the same magnetic field. These authors obtained for the ratio of the Bohr magneton to the proton magnetic moment:

$$\frac{\mu_0}{\mu_{p\ (\text{oil})}} = 657.475 \pm 0.008. \tag{2.14}$$

The subscript to the proton magnetic moment indicates that its value was obtained from measurements on a spherical sample of mineral oil.

The second experiment was carried out by Koenig, Prodell and Kusch[59] who obtained the ratio of the electron magnetic moment to the proton magnetic moment. The first was achieved by measuring transitions in hydrogen atoms, while the latter, once again, involved the measurement of the proton resonance frequency in mineral oil. Both measurements were carried out in the same magnetic field and yielded the ratio

$$\frac{\mu_e}{\mu_{p\ (\text{oil})}} = 658.2288 \pm 0.006. \tag{2.15}$$

The combination of these two results yielded[59]

$$\frac{\mu_e}{\mu_0} = 2\,(1.001146 \pm 0.000012), \tag{2.16}$$

or

$$a_e = (1.146 \pm 0.012)\cdot 10^{-3}.$$

The measurement of $\mu_e/\mu_{p\,(\text{oil})}$ was later confirmed by Beringer and Heald[60] who obtained

$$\frac{\mu_e}{\mu_{p\ (\text{oil})}} = 658.2298 \pm 0.0002, \tag{2.17}$$

but a repetition of the measurement of $\mu_0/\mu_{p\,(\text{oil})}$ by Franken and Liebes[61] gave a value slightly shifted from that given in Eq. (2.14). The new result and the value of g which was deduced from it were

$$\begin{aligned} \frac{\mu_0}{\mu_{p\ (\text{oil})}} &= 657.462 \pm 0.003, \\ g &= 2\,(1.001168 \pm 0.000005). \end{aligned} \tag{2.18}$$

Comparison with Eq. (2.9) indicates that this second result is somewhat closer to the present-day theoretical prediction than the first result given in Eq. (2.16).

The advantage of the measurements in hydrogen was that there were no electron-electron interactions to take into account, and the correction due to the relativistic increase in the mass of the electron, bound in the hydrogen atom, was small. The actual correction factor is:

$$g = g_J\left(1+\frac{\alpha^2}{3}\right) \tag{2.19}$$

to second order in the fine structure constant α, and thus g and the measured quantity g_J only differ by about 18 parts per million (18 ppm). However, it was apparent that even in the simplest atomic system the accuracy in the measurement of the electron g-factor was seriously limited. The route to a more stringent test of quantum electrodynamics lay through experiments conducted on free electrons. When reviewing these developments Kusch[5] stated: "Once again in the history of physics, a new technique may yield results of far greater precision than any visualizable extension of older techniques." We shall see how in the history of the g-factor measurements such a jump in precision occurs on more than one occasion. In order to understand the way in which these experiments have evolved we start with some general considerations before tracing the development of specific techniques.

The solution of the Dirac equation for the motion of a free electron in a uniform magnetic field $[\vec{B}=(0,0,B_z)]$ was given by Rabi[62] in 1928, and the relativistic form of the associated energy eigenvalues can be written

$$E=\sqrt{m_0^2c^4+p_z^2c^2+(2n+1+gm_S)\cdot 2\mu_0 B m_0 c^2}, \tag{2.20}$$

where $n=0,1,2,\ldots$ is the orbital quantum number and $m_s=\pm\frac{1}{2}$ that for the spin of the electron. The component of the electron momentum in the direction of the magnetic field, p_z, is not constrained and so may take on a continuum of values. For non-relativistic velocities the energy can be expressed approximately as

$$E-m_0c^2=\frac{p_z^2}{2m_0}+(2n+1+gm_S)\,\mu_0 B. \tag{2.21}$$

If g were exactly equal to 2, then the second term on the right of this equation could be compressed to the form $2j\mu_0 B$, with j taking the values 0, 1, 2, etc. In this case there is one set of energy levels, all doubly degenerate except for the lowest $(j=0)$ which is single. Here we have neglected the continuum of allowed p_z values. This is just the solution obtained by Rabi[62] since, as we have noted above, the Dirac equation does give $g=2$. If the anomalous part of g is taken into account and $g=2(1+a_e)$ is inserted into Eq. (2.21), then the degeneracy is lifted and there are essentially two sets of energy levels (Rabi-Landau levels) for the two assignments of the spin quantum number. The energies for these two sets of levels can be written as

$$(2n-a_e)\,\mu_0 B.\quad [2(n+1)+a_e]\,\mu_0 B, \tag{2.22}$$

with $n=0,1,2,\ldots$ as before. These levels are shown in Fig. 2.

There are several features that should be noted. Transitions between adjacent levels within either of these sets occur at the frequency

$$\frac{2\mu_0 B}{\hbar}=\frac{eB}{m_0 c}=\omega_0. \tag{2.23}$$

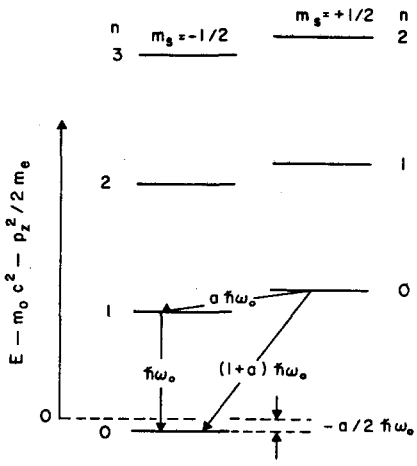

FIG. 2. Rabi-Landau levels of an electron in a uniform magnetic field B. $\omega_0=eB/m_ec$.

Spin-flip transitions imply a change from one set of energy levels to the other while the orbital quantum number n remains constant. These occur at the Larmor frequency

$$\frac{g\mu_0 B}{\hbar}=\frac{g}{2}\,\omega_0=\omega_L. \tag{2.24}$$

The combination of a change by one unit in the orbital quantum number and a spin flip would involve a frequency which is directly proportional to the anomalous part of the g-factor:

$$\frac{2a_e\mu_0 B}{\hbar}=a_e\omega_0=\omega_a. \tag{2.25}$$

These basic transitions and their associated frequencies are given in Table 2.2.

As mentioned above, the lowest level for the case g exactly equal to 2 is a singlet; it is also non-magnetic in that $j=0$ and there is no term, in the expression for the energy, which comes from the magnetic field. When the anomalous part of the g-factor is included, however, this level is depressed to the negative value $-a_e\mu_0 B$ while all the other levels remain positive. Thus if the electrons are in a non-uniform magnetic field, then when they move towards regions of lower field those in the very lowest level will experience a slightly rising potential energy barrier, while in all other states the magnetic field contribution to the energy acts like a downhill potential gradient. Thus a slightly non-uniform magnetic field can be used as a filter for those electrons in the very lowest state.

Finally an examination of the eigenfunctions for the simple zero velocity case[63] indicates that while the expectation value of the component of the spin in the direction of the magnetic field remains constant for an

TABLE 2.2. Frequencies of the transitions between Rabi-Landau levels.

Δn	Δm_S	$\lvert\Delta E\rvert$
0	±1	$(1\mp a_e)\,\hbar\omega_0=\hbar\omega_L$
±1	0	$\hbar\omega_0$
±1	±1	$a_e\hbar\omega_0=\hbar\omega_a$

electron in a given state, the component in the xy plane precesses with the Larmor frequency ω_L.

For a particle with finite velocity the spin rotation is reduced by the relativistic Thomas precession (ω_T), which is given by

$$\omega_T = \frac{\gamma - 1}{\gamma} \frac{eB}{m_0 c} = \frac{\gamma - 1}{\gamma} \omega_0, \tag{2.26}$$

where $\gamma = (1 - \beta^2)^{-1/2}$ with β the particle velocity divided by the velocity of light and, to keep the discussion simple, we consider circular motion in the xy plane; that is we continue to neglect p_z. The net angular rotation frequency of the spin in the laboratory is then

$$\omega_S = \omega_L - \omega_T = \frac{g}{2} \omega_0 - \frac{\gamma - 1}{\gamma} \omega_0 = \left(a_e + \frac{1}{\gamma}\right) \omega_0. \tag{2.27}$$

The cyclotron frequency of the electron in its circular orbit also depends on the particle velocity and can be written

$$\omega_c = \frac{eB}{\gamma m_0 c} = \frac{\omega_0}{\gamma}. \tag{2.28}$$

This is just the relativistic equivalent to Eq. (2.23). It also represents the frequency with which the electron momentum rotates in the laboratory frame. By comparing Eqs. (2.27) and (2.28) we can see that the anomaly a_e causes the spin to rotate at a slightly higher frequency than the momentum vector, the difference frequency being independent of γ, or the particle velocity, and just equal to the ω_a of Eq. (2.25):

$$\omega_S - \omega_c = a_e \omega_0 = \omega_a. \tag{2.29}$$

Thus the expectation value of the longitudinal component of the electron spin oscillates back and forth with this frequency as the particle moves in a uniform magnetic field.

This simple discussion has illustrated the two experimental techniques which have been used to determine the lepton g-factor of free particles. They are (i) the spin resonance experiments on slow electrons in which the frequencies of transitions between the Rabi-Landau levels, given in Eq. (2.22), are observed, and (ii) the precession method in which the evolution of the longitudinal polarization with time is observed for an initially polarized ensemble of particles. The spin resonance method is related to that of resonantly inducing transitions, between the Zeeman levels of an atom in a magnetic field except that, rather than being confined in the relatively strong Coulomb field of the nucleus, the electron is in this case only very weakly bound by a shallow trapping potential. By this means the relativistic corrections are minimized, and effects due to the trapping itself are kept small and calculable.

An early proposal for an experiment of this type was that of Bloch[64] who, in 1953, reported the investigation of a scheme to trap electrons in a potential well of depth about 10^{-5} V superimposed on a magnetic field of 0.1 T. The basic idea was that a non-uniform magnetic field would by cyclically applied in addition to the uniform one, and that its strength would be sufficient to eject from the electric field trap all but those electrons in the lowest Rabi-Landau level. Between applications of this non-uniform field the radio-frequency power would be applied. The resonantly induced transitions into the higher energy levels would then be signalled by electrons leaving the trap at the next application of the non-uniform magnetic field. No measurement of the anomaly resulted from this proposal nor from the earlier one of Tolhoek and De Groot[65] in which the resonant depolarization of electrons was to be studied by interposing a uniform magnetic field and an RF field between two Mott scatterers. Thus this experiment was to use the fact, originally pointed out by Mott,[66] that electrons scattered from a nucleus emerge with partial polarization perpendicular to the plane of scatter. In a second scattering process such a partially polarized beam would then exhibit an azimuthal dependence of the intensity. It was not proposed to trap the electrons and so it is doubtful whether sufficient time would elapse between polarization and analysis for a well-defined frequency to have been measured.

The first determination of the anomalous part of g with free electrons was made by Dehmelt in 1958.[67] An applied RF field induced spin resonance transitions on free electrons in a magnetic field. The electrons were in a buffer gas and were polarized by means of collisions with polarized sodium atoms. The value obtained for the electron anomaly was

$$a_e = (1.116 \pm 0.040) \cdot 10^{-3}. \tag{2.30}$$

The next stage in the evolution of the spin resonance method was the development of the Penning[68] trap in the form described by Pierce.[69] The trap, in which hyperbolic electrodes provide the trapping potential in the direction of the magnetic field lines, was used by Dehmelt[70] for cyclotron resonance and thermalization studies on electrons. We will discuss the main features of the trap in the latter part of this section when we deal with the most recent spin resonance experiments and results. However, in this early work no spin resonance signal was observed.

Following a similar approach of using the Penning trap in conjunction with a sodium beam for polarization and analysis of the stored electrons, Gräff, Major, Roeder and Werth[71] reported the detection of the spin and cyclotron resonance signals in 1968. This was followed by the first observation of the electron $(g-2)$ resonance by Gräff, Klempt and Werth[72] who were thus able to measure the electron anomaly directly, for which they obtained

$$a_e = (1\,159\,660 \pm 300) \cdot 10^{-9}. \tag{2.31}$$

The precision of this result was limited by the large linewidth of the resonance and at this stage the spin resonance method was not proving as tractable or as accurate as the precession method.

This situation was dramatically changed recently when Dehmelt and his co-workers managed to hold single electrons in a trap. With this so-called monoelectron oscillator[73] the $(g-2)$ spin-flip transitions of a solitary electron have been observed and the most accurate value of the electron anomaly obtained. We discuss the experiment in more detail below.

The evolution of the precession method occurred very much in parallel with that of the spin resonance techni-

ques. Subsequent to the experiments on atoms, a step forward in opening up the possibilities of achieving higher precision had been made in 1953 in Louisell, Pidd and Crane[74] measured the precession frequency of the spin of a free electron in a magnetic field. The electrons were polarized by Mott scattering and then passed into a magnetic field region in which their trajectories spiralled and their spins precessed with the frequency given in Eq. (2.27). It should be noted that the electrons had a kinetic energy of 400 keV and were consequently relativistic. The Thomas precession (ω_T) was approximately 40% of the Larmor frequency (ω_L). The experiment, with its accuracy of the order of 10%, did not clearly demonstrate that g was greater than 2, but it had shown that it was possible to measure the g-factor of a free electron.

An improved precision was reached in the second Michigan experiment in which Schupp, Pidd and Crane[75] reported modifications to the technique. Instead of measuring the total spin rotation in the magnetic field between polarizer and analyser, they measured the differential rotation of the spin with respect to the electron velocity vector. This experiment gave birth to what is now called the $(g-2)$ precession measurement technique, and it led to a significant jump in the precision with which the g-factor was measured. We have seen the reason for this above in Eq. (2.29), which shows that the difference between the spin precession frequency and the cyclotron frequency of the electron orbit is directly proportional to the anomalous part of the magnetic dipole moment. Thus a direct attack was made on the anomaly itself rather than on the g-factor. Another improvement in the technique embodied in this experiment was that a magnetic bottle was used to trap the electrons, thereby allowing their spins to precess through many revolutions before the polarization was analyzed. The final result of this experiment was

$$a_e = (1160.9 \pm 2.4)\cdot 10^{-6}. \tag{2.32}$$

As we have said, this experiment laid down the basis of the $(g-2)$ technique with which highly precise measurements of the g-factors of both the electron and the muon have subsequently been made. The sequence of experiments carried out at Michigan on the electron has been described in a review by Rich and Wesley.[1] The precision was successively increased until, in the latest measurement done in high magnetic field, Wesley and Rich[76] obtained an accuracy of 3 ppm. The result of this experiment was

$$a_e = (1\ 159\ 656.7 \pm 3.5)\cdot 10^{-9}, \tag{2.33}$$

where we have included the small correction calculated by Granger and Ford.[77]

Experiments on the positron have also been carried out by the Michigan group. In this case the initial polarization was obtained by using a radioactive source of positrons, and at the end of the storage period the final polarization was based on positronium formation[78] in a plastic scintillator immersed in a magnetic field. For this latter the optimum field strength is 1 T, while in the trapping region the uniform magnetic field was only 0.1 T. The consequent necessity to separate these two field regions placed some limitations on the precision of the measurement. Full details of the experiment are given by Gilleland and Rich,[79] who quote the result

$$(\text{positrons})a_e = (1160.3 \pm 1.2)\cdot 10^{-6}. \tag{2.34}$$

It should be noted that this is the most precise current value for the positron. That there is a factor of a thousand between this precision and that for the electron reflects the comparative difficulty of the two experiments. The accuracy of the positron experiment is limited by counting statistics, the number of positrons trapped per cycle being some 7 orders of magnitude less than for electrons. This disadvantage is somewhat offset by the more efficient polarization analysis in the positron experiment. The Michigan group have also performed a novel type of resonance experiment. Although the preliminary result obtained by Ford, Luxon, Rich, Wesley and Telegdi[80] was limited in precision to some 100 ppm, the method shows great promise for an improved measurement of the positron anomaly.

The novel feature of the experiment was that the spin was resonantly perturbed by passing an RF current of frequency ω_a down a wire which was parallel to the uniform magnetic field direction. Such an RF field, symmetrical about the axis of the trapping region, exactly matches the precession of the spin relative to its momentum. Under this resonant condition the electron experiences a torque which rotates its spin towards the direction of the constant magnetic field. Continuous application of the RF will cause the spin to rotate through that direction and back to its original plane of precession. Thus the asymmetry in the second Mott scatter can be made to disappear and then reappear. The advantage of this technique as far as the positron experiment is concerned is that a spin parallel to the magnetic field is just the orientation which is required if the polarization analysis is to be carried out by means of positronium formation in the same magnetic field.

Such an experiment is in preparation, and details have been given by Newman, Sweetman and Rich[81] together with those of an improved version of the electron precession apparatus.

The precession method has also been employed in the measurement of the g-factor of the muon, the principal difference being the procedure for obtaining the initial longitudinal polarization and analyzing its evolution as a function of time. There is a further important difference and this arises from the fact that the muon is an unstable particle. Clearly the more periods of the $(g-2)$ oscillation that can be observed the more accurate will be the determination of ω_a. This can readily be seen by considering that n periods of the oscillation, extending over a measured time of t, are counted with an uncertainty of one cycle. The frequency is then $(n/t) \pm (1/t)$ and its error decreases as the duration of the measurement t increases. Thus it is of advantage to store the particles in the uniform magnetic field region for as long as possible. In the case of the electron experiments this time is only limited by the quality of the trap, but for muons it is seriously curtailed by the life-

time. To lessen this restriction it is necessary to use the relativistic dilation of the decay time which results from going to higher particle energies. Real gains can be made since, as can be seen from Eq. (2.23) and (2.29), the frequency ω_a does not depend upon the particle energy; the muon lifetime can therefore be stretched out to cover more and more periods of the relative spin precession.

Before the first muon $(g-2)$ precession experiment was carried out at CERN,[82] the evidence for an anomalous g-factor of the muon was indirect. It came from a combination of a measurement of the Larmor spin precession frequency [Eq. (2.24)] for muons at rest in a known magnetic field[83] with the measurement of the muon mass obtained from observations of the 88 keV $(3d-2p)$ X-ray transition in muonic phosphorus.[84,85] By substitution of this latter in Eq. (2.23) the value of ω_0 for the particular magnetic field used in the precession experiment could be found, and then the g-factor followed from Eq. (2.24). The result was

$$g_\mu = 2\,(1.001^{+0.0001}_{-0.0002}), \tag{2.35}$$

where the errors largely reflect the uncertainty in the muon mass which at that time was about ±100 ppm.

The effect of such an uncertainty can be reduced, as we have seen, by making a direct measurement of the anomaly through ω_a. That is, we combine Eq. (2.23) with Eq. (2.25) instead of Eq. (2.24). The precedent had been set in the electron experiment of Schupp, Pidd and Crane,[75] and the first muon $(g-2)$ experiment was carried out soon afterwards at the CERN synchro-cyclotron by Charpak, Farley, Garwin, Muller, Sens, Telegdi and Zichichi.[82] This was the first in the sequence of CERN muon experiments.

All three of these experiments used muons from pion decay $\pi^+ \to \mu^+ + \nu_\mu$. Parity non-conservation in this process provides the initial polarization of the muons in the following way. In the pion rest frame the muons have a longitudinal polarization of 100%. Thus if muons which are produced close to the forward direction are selected, then this yields a beam with high initial longitudinal polarization in the laboratory. Such muons are at the top of the allowed momentum range, and so by matching the momentum of the original pion beam with that of the selected muons, a sample of the latter can be obtained with over 95% initial polarization.

The analysis of the longitudinal polarization as a function of the time which the muon spends in the magnetic field, is effected by making use of the asymmetry in the electron angular distribution, with respect to the muon spin direction, which arises from parity non-conservation in the muon decay process $\mu^+ \to e^+ + \nu + \bar{\nu}_\mu$. Access to this asymmetric distribution may be obtained directly by stopping the muons and thereby going to the muon rest frame, or by applying an energy cut on the detected electrons from decay in flight. The first CERN muon experiment used the former method, while the subsequent two experiments employed the detection of decays in flight. The process of applying an energy cut on these electrons is equivalent to selecting those which go forward in the muon rest frame. The number of decay positrons in this high energy group will be high or low depending on whether the muon spin is pointing forwards or backwards with respect to the muon direction. As we have mentioned above, the expectation value of the longitudinal component of the muon spin oscillates with the $(g-2)$ frequency and consequently the count rate of the selected decay electrons will be modulated with this frequency ω_a.

In the first CERN experiment[82] a longitudinal polarized muon beam was formed by forward decay of pions in flight inside the cyclotron. Scattering in a beryllium moderator reduced the muon momentum to 90 MeV/c and also injected the particles into the gap of a 6 m magnet. The 1.6 T field of this magnet was so shaped that the muon orbits slowly drifted down its length, making up to 1000 turns before reaching the ejection region. The final polarization was measured by stopping the muons in a nondepolarizing target, situated beyond the magnetic field region, and then detecting the forward-backward asymmetry in the decay electron distribution. This first measurement of the anomalous part of the g-factor of free muons was obtained from data containing about a million stopped muons, and yielded the result

$$a_\mu = (1162 \pm 5)\cdot 10^{-6}. \tag{2.36}$$

This number was of similar precision to and in excellent agreement with the theoretical value at that time.

The second CERN muon experiment[86] brought the considerable improvement of trapping the muons in a weak focusing storage ring. The pions which decayed to give the stored muons were themselves produced when a 10 GeV proton beam struck a target situated inside the storage ring magnetic field but outside the storage volume itself. Because of this procedure the stored muons, which had a momentum of 1.27 GeV/c, were derived from pions with a fairly broad band of energies and consequently the initial polarization of the sample was fairly low (26%). The pions were not on stored trajectories, and the higher energy ones quickly left the magnetic field region while those with momenta closer to 1.27 GeV/c would travel some distance around the ring and thus have a higher probability of producing a stored muon. The perturbation essential for injecting the muons on to closed orbits was provided by the decay process in which the neutrino carried off some of the momentum. In just a few cases the momentum and direction of the remaining muon was within the acceptance of the storage ring.

The lifetime of the stored muons with momenta 1.27 GeV/c is increased over the value at rest, of 2.2 μsec, by the relativistic time dilation factor $\gamma \sim 12$. The relative precession of the muon spin with respect to its momentum vector was followed, as a function of time spent by the muon in the magnetic field, by energy selection of the decay electrons as discussed above. The stretching of the muon lifetime by time dilation enabled some 50 cycles of the $(g-2)$ oscillations to be observed in the time spectrum of decay electron counts. The frequency obtained from this data was then converted into a value for the anomaly by using the magnetic field strength which had been measured in terms of the pro-

ton magnetic resonance frequency in the field. In order to complete this conversion, the ratio of the muon precession frequency at rest to the proton magnetic resonance frequency is also required.

It should be noted that in a weak focusing ring the magnetic field is made nonuniform in order to contain the particle orbits vertically. There is a gradient in the field, and consequently any uncertainty in the position of the muon orbits leads to an uncertainty in the mean value of the magnetic field seen by the stored sample. This is just an example of how the need to trap the particles conflicts with the aim of observing the spin motion in a precisely known magnetic field. The final error for this experiment[86] contained a large contribution due to this source. The experimental value obtained for the anomaly was

$$a_\mu = (1166160 \pm 310)\cdot 10^{-9}, \tag{2.37}$$

in good agreement with the theoretical expectations expressed in Eq. (2.9).

This experiment was the progenitor of the third and most recent CERN muon experiment[87,88]; they share many common features, as will become clear from the discussion below.

2.3 Measurement of the muon anomalous magnetic moment by the precession method

In this and the following sections we will discuss the recent experiments to measure the anomalous parts of the muon and electron g-factors by the precession and spin resonance methods, respectively. These two experiments are of vastly different scales; the electrons have non-relativistic energies in the region of one milli-electron volt, while the muons are highly relativistic with energies of about 3.1 GeV. The electrons are trapped on cyclotron orbits of radii ~1 μm and oscillate vertically over a distance of about 200 μm, while the muons, travelling virtually at the velocity of light, follow near circular orbits of 7 m radius and execute vertical oscillations over a range of up to 80 mm. There is little doubt that the macroscopic nature of the motion of the many millions of muons which contribute to the measured signal, but in the mono-electron oscillator a single electron spends a sizeable part of its time in the lowest quantum level of the system.

These differences are largely dictated by the need to use the relativistic time dilation of the muon lifetime on the one hand and to minimize the frequency shift due to the electron trapping potential on the other: in spite of them there are strong similarities between the two experiments; in particular, the use of a type of Penning trap is common to both. The trap consists of an electric quadrupole superimposed upon a uniform magnetic field. Both the configurations used in these two experiments have axial symmetry, and a general form for the electric potential in cylindrical coordinates is

$$V(r, z) = \frac{V_0}{b^2}[r^2 - 2r_0^2(\ln r - \ln r_0) - r_0^2 - 2z^2], \tag{2.38}$$

where r_0 is the radius of the circle at which $\partial V/\partial r = 0$. The potential is singular along the symmetry axis except in the case when $r_0 = 0$. At this limit the form of the potential becomes

$$V(r, z) = \frac{V_0}{b^2}(r^2 - 2z^2), \tag{2.39}$$

which is just the potential of the electron trap and is discussed further below.

For the muon experiment, as we have mentioned above, r_0 is 7 m and the particle orbits are restricted by the aperture limits to radii within ±60 mm of this value and also to within ±40 mm of the horizontal plane $z = 0$. Thus by writing $r = r_0 + x$ the potential can be approximately reduced to the two-dimensional form

$$V(x, z) = \frac{2V_0}{b^2}(x^2 - z^2), \tag{2.40}$$

which completely neglects the effects of curvature. Thus in cross-section the shape of the four electrodes, required to provide the quadrupole field, closely resembles that which satisfies the simple two-dimensional case, but perpendicular to this section the electrodes are curved to follow the circumference of the 7 m radius ring.

In both the electron and muon traps the classical motion of the particles can be described in the same terms as a combination of three frequencies. The first is the relatively fast cyclotron frequency due to the magnetic field but slightly modified by the trapping potential so that the orbits are not quite circular. The center of the cyclotron orbits can be considered to slowly drift around the axis of symmetry such that the particle executed an epitrochoidal motion, the frequency of this drift being the so-called magnetron motion. In the case of the muon storage ring the size of the horizontal aperture always ensures that the center of the 7 m radius cyclotron orbit is always within 60 mm of the symmetry axis or center of the ring. The third frequency is that of the vertical oscillations in the direction of the magnetic field. This latter frequency and the magnetron frequency both go to zero in the absence of a trapping potential.

It should be remembered that strictly speaking this classical approximation is not applicable to the quantum states of the electron in the mono-electron oscillator.

Now concentrating on the muon experiment we write out the classical relativistic equations of motion for the chosen configuration of transverse fields ($\beta \cdot \mathbf{B} = \beta \cdot \mathbf{E} = 0$):

$$\frac{d\beta}{dt} = [\omega_c \beta], \quad \frac{d\sigma}{dt} = [\omega_S \sigma], \tag{2.41}$$

where ω_c and ω_s are shifted from the values given in Eqs. (2.28) and (2.27) owing to the presence of the electric field. They are now given by

$$\omega_c = \frac{e}{m_0 c}\left(\frac{\mathbf{B}}{\gamma} - \frac{\gamma}{\gamma^2 - 1}[\beta \times \mathbf{E}]\right), \tag{2.42}$$

$$\omega_S = \frac{e}{m_0 c}\left\{\left(a + \frac{1}{\gamma}\right)\mathbf{B} + \left(\frac{1}{\gamma^2 - 1} - a - \frac{\gamma}{\gamma^2 - 1}\right)[\beta \times \mathbf{E}]\right\}, \tag{2.43}$$

in which the additional electric field terms are evident. These terms mean that the relative precession of the spin with respect to the momentum is now not exactly at the frequency ω_a of Eq. (2.29). Writing this shifted frequency at ω_a' we have

$$\omega_a' \equiv \omega_S - \omega_c = \frac{e}{m_0 c}\left\{ aB + \left(\frac{1}{\gamma^2-1} - a\right)[\beta \times E]\right\}$$
$$= \omega_a + \frac{e}{m_0 c}\left(\frac{1}{\gamma^2-1} - a\right)[\beta \times E]. \quad (2.44)$$

This equation emphasizes the point that the trapping potential shifts the observed frequency from the desired value ω_a. It is also clear that this shift is zero for the special choice of particle energy equivalent to

$$\gamma = \sqrt{1+\frac{1}{a}} = 29.3. \quad (2.45)$$

For muons this is equivalent to a momentum of 3.098 GeV and it is at this value that the muon storage ring is designed to operate.

In practice, of course, the magnetic field is not completely uniform and there is some spread in the particle momentum (±0.7%) about the central "magic" value, but the net result of this choice of fields and muon momentum is that the uncertainties in obtaining the muon anomaly from the measured precession frequency are reduced to the level of a few parts per million.

The experiment was mounted by a CERN-Daresbury-Mainz Collaboration.[87,88] Technical details are given in these references and also in the reviews listed in Ref. 1. We therefore limit ourselves to a brief summary of the main features.

A plan view of the storage ring is shown in Fig. 3. At each cycle of the CERN Proton Synchrotron a pion beam with momentum spread of ±0.75% is injected into the volume where the muons are to be stored by means of a pulsed inflector. The pions have slightly higher momentum than the 3.098 GeV/c for which the magnetic field of the storage ring is set. Consequently they tend to leave the ring on the outside, but before they do so about a tenth of them decay. The overall trapping efficiency of stored muons produced per injected pion is about 10^{-4}. The advantage of this method of producing the stored muon population is that the sample has high initial polarization in excess of 90% owing to the fact that the muons are selected from the top 1.5% of the available momentum range and hence maximum use is made of the complete polarization of the muons in the pion rest frame. We have already discussed the crucial role that parity nonconservation plays in both the provision and detection of the muon polarization.

As can be seen from Fig. 3 the storage ring consisted of 40 bending magnetis placed around the circumference of a ring of 14 m diameter. The magnets were C-shaped in section with their open sides towards the center of the ring, and had pole pieces so shaped that their ends fitted together to form a 40-sided polygon.

The electrodes (also shown in cross-section in Fig. 3), which provided the trapping potential for the vertical motion of the particles, were mounted inside vacuum tank sections which each covered a sector of the ring equivalent to four magnet blocks in length. To accomodate the pion inflector a complete sector was left free of electrodes, and in order to keep the closed orbit distortion to a minimum the sector diametrically opposite the inflector was also left without electric field.

The decay electrons were detected by 22 energy-sensitive shower counters spread evenly around the inside of the ring. The time spectrum of the recorded counts is displayed in Fig. 4. The characteristic exponential decay can clearly be seen, as can the modulation at the $(g-2)$ frequency which is due to the selection of the larger pulse heights; that is, just the application of an energy cut on the decay electrons as discussed above.

In order to apply the small corrections due to the slight inhomogeneity of the magnetic field and the effect of the electric field, it is necessary to know how the muon momenta or equilibrium orbits are distributed. This is measured by observing the rotation of the narrow (10 nsec) bunch of muons around the ring just after injection. At this early time the decay electron time spectrum clearly shows the rotating bunch, and the way in which this bunch disperses in time is used to obtain the momentum distribution.

The value of ω_a obtained from the data, as shown in Fig. 4, was converted into a value of the anomaly by means of the magnetic field measurements. These were made at about a quarter of a million points throughout the storage volume both before and after a sequence of runs. The field values were obtained in terms of the proton magnetic resonance frequency and, after averaging over the muon equilibrium orbit distri-

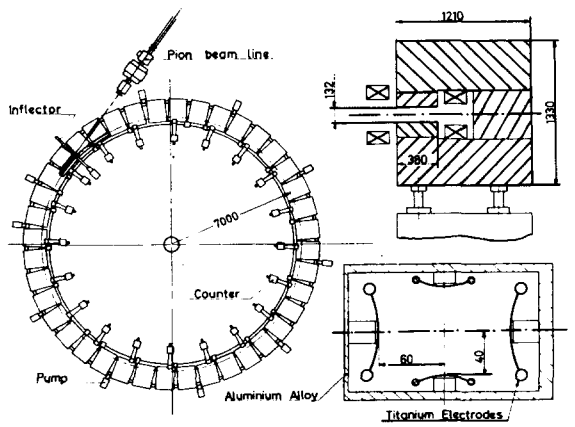

FIG. 3. Plan view of the second CERN muon storage ring, with cross-sections of the magnets and focusing electrodes. Dimensions in mm.

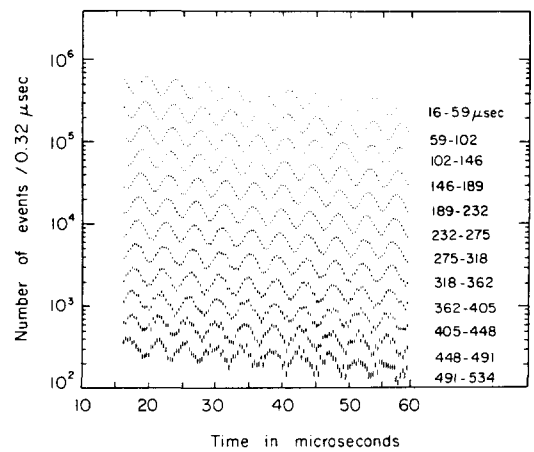

FIG. 4. Decay electron time distribution from the CERN muon $g-2$ experiment. The distribution contains 1.4×10^8 events.

bution and applying corrections for shielding and calibration of the probes, the resulting mean magnetic field seen by the muon sample was expressed in terms of the effective mean Larmor frequency of protons in vacuum. The overall average value of R, the ratio of the $(g-2)$ frequency to this effective mean Larmor frequency, was[88]

$$R = 3.707213(27)\cdot 10^{-3}. \tag{2.46}$$

The final step in obtaining the anomaly a_μ requires the ratio λ of the Larmor frequency of the muon to that of the proton (or equivalently the ratio of their magnetic moments). Recent measurements of this ratio have been made by Crowe *et al.*[89] and Casperson *et al.*[90] The two values are in good agreement, and the weighted average is

$$\lambda = 3.1833417(39), \tag{2.47}$$

which, when inserted into the equation

$$a_\mu = \frac{R}{\lambda - R} \tag{2.48}$$

gives the results[45]

$$a_{\mu^+} = (1\,165\,912 \pm 11)\cdot 10^{-9},$$
$$a_{\mu^-} = (1\,165\,938 \pm 12)\cdot 10^{-9}. \tag{2.49}$$

which together provide the average experimental value of the muon anomaly,

$$\text{experiment:}\quad a_\mu = (1\,165\,924 \pm 8)\cdot 10^{-9}, \tag{2.50}$$

in excellent agreement with the theoretical prediction quoted in Eq. (2.9):

$$\text{theory:}\quad a_\mu = (1\,165\,920 \pm 10)\cdot 10^{-9}.$$

2.4 Measurement of the electron anomalous magnetic moment by the spin resonance method

2.4.1 Ideal Penning trap

As we have mentioned above, excellent reviews of experiments employing this technique have been given in the articles of Rich and Wesley and of Dehmelt listed under Ref. 1.

We will discuss the recent experiment carried out on the electron at the University of Washington by Dehmelt and his co-workers [73,91,92]

In general, as we have seen, the measurements of the lepton g-factors are made on leptons trapped in a region of homogeneous magnetic field, and in order that the measurement may be made at high precision it is necessary that the additional field which provides the trapping should not greatly perturb the system.

In this experiment the electrons are confined within a Penning trap which, as we have noted in the previous section, takes the form of a uniform magnetic field of 18.3 kG with a cylindrically symmetric electric quadrupole field superimposed. The electric potential $V(r, z)$ has the form given in Eq. (2.39):

$$V(r, z) = \frac{V_0}{b^2}(r^2 - 2z^2).$$

This potential is provided by two end caps ($V = -V_0$) shaped to the surfaces, $z_s^2 = \frac{1}{2}(r^2 + b^2)$, and a ring electrode ($V = +V_0$) which has the shape $r_s^2 = b^2 + 2z^2$; the dimension b equals 0.473 cm.

The nonrelativistic Hamiltonian for the particle, including the spin-dependent part, is given by

$$\mathcal{H} = \frac{\mathbf{P}^2}{2m_0} - eV + \mu_0 \frac{g}{2}(\sigma \mathbf{B}), \tag{2.51}$$

where the kinetic momentum operator has the minimal coupling form

$$\mathbf{P} = -i\hbar\nabla + e\frac{\mathbf{A}}{c}. \tag{2.52}$$

For a uniform magnetic field $\mathbf{B} = (0, 0, B_z)$, the vector potential is

$$\mathbf{A} = \left(-y\frac{B_z}{2},\ x\frac{B_z}{2},\ 0\right). \tag{2.53}$$

The Schrödinger equation with this Hamiltonian has been solved by Sokolov and Pavlenko,[93] and the eigenvalues are given in terms of the integer quantum numbers n, n_z, and n_m, and the spin quantum number m_s by

$$E = \hbar\left[\left(n + \frac{1}{2}\right)\omega_c' + \left(n_z + \frac{1}{2}\right)\omega_z - \left(n_m + \frac{1}{2}\right)\omega_m + \omega_L m_S\right],$$
$$n,\ n_z,\ n_m = 0,\ 1,\ 2\ \ldots;\ m_S = \pm\frac{1}{2}. \tag{2.54}$$

The first term involves the cyclotron orbital motion at the modified frequency given by

$$\omega_c' = \frac{eB}{m_0 c} - \omega_m = \omega_0 - \omega_m, \quad \frac{\omega_c'}{2\pi} \approx 51\ \text{GHz}. \tag{2.55}$$

The second term is due to the quantized axial oscillations whose fundamental frequency depends only upon the electrostatic field,

$$\omega_z = 2\sqrt{\frac{V_0 e}{m_0 b^2}}, \quad \frac{\omega_z}{2\pi} \approx 59\ \text{MHz}. \tag{2.56}$$

The third term represents the contribution to the energy from the magnetron oscillation which is slow in comparison with the cyclotron motion. In this ideal axially symmetric trap the center of the cyclotron orbit circulates around the x-axis with the frequency

$$\omega_m = \frac{\omega_0}{2}\left(1 - \sqrt{1 - \frac{2\omega_z^2}{\omega_0^2}}\right), \quad \frac{\omega_m}{2\pi} \approx 34\ \text{kHz}. \tag{2.57}$$

With the aid of Eq. (2.55) this latter equation can be rearranged into the useful form

$$2\omega_c'\omega_m = \omega_z^2. \tag{2.58}$$

The final term in Eq. (2.54) is just the energy due to the two possible orientations of the electron spin with respect to B_z (i.e., $m_s = \pm\frac{1}{2}$).

If the frequencies ω_z and ω_m are to remain real we can deduce from Eqs. (2.56) and (2.57) the inequality

$$0 < \frac{eV_0}{b^2} < \frac{e^2B^2}{8mc} \tag{2.59}$$

which defines the domain of the applied voltage V_0 for which the electron will remain confined within the trap. The lower limit has to be satisfied in order that the vertical motion is stable while the upper limit ensures stability of the radial motion.

In the limit of an extremely weak trapping potential ($V_0 \to 0$) the energy eigenvalues reduce to the Rabi-Landau levels [cf. Eq. (2.21) et seq.]:

$$E = \hbar\omega_0\left(n + \frac{1}{2} + \frac{g}{2}m_S\right). \tag{2.60}$$

We have seen from Eqs. (2.23) and (2.25) that the determination of the anomaly a_e involves the measure-

ment of the ratio of the frequencies ω_a and ω_0. In terms of the frequencies discussed above, this ratio can be written

$$a_e = \frac{\omega_a}{\omega_0} = \frac{\omega_a' - \omega_m}{\omega_c' + \omega_m}, \tag{2.61}$$

where $\omega_a' = \omega_L - \omega_c'$. Thus the necessity of trapping the electrons means that in effect three frequencies have to be measured in order to obtain a_e. In practice these frequencies are ω_c', ω_a', and ω_z, from which ω_m may be deduced by means of Eq. (2.58).

2.4.2 Single electron trap

The remarkable feature of this experiment is that measurements are made on a *single electron* confined in the trap. Electrons (produced inside the trap by ionization of residual gas atoms by an electron beam) are detected by applying an RF voltage to the lower focusing cap (see Fig. 5). The induced axial motion of a single electron then gives a detectable signal at the upper cap ($\simeq$0.1 μV per stored electron). If the applied RF voltage is raised above ~2 mV, electrons are driven from the trap,[73] the loss of each electron being signalled by a step in the voltage detected at the upper cap. This process is continued until this voltage corresponds to a single stored electron. The amplitude of the applied RF is then reduced, and measurements can be made on the single trapped electron for periods of several days.

The methods employed to measure the three frequencies ω_z, ω_c', and ω_a, needed to find the anomaly a_e, are now described.

2.4.3 Axial oscillation frequency ω_z

This frequency is maintained at a constant value throughout the experiment by means of a feedback loop. The signal induced on the upper cap by the axial motion of the electron is combined with the input drive voltage to give an error signal depending on the frequency difference between the detected and drive frequencies.

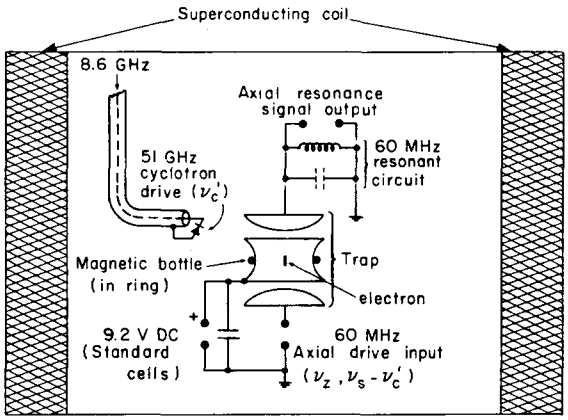

FIG. 5. Schematic of the University of Washington experiment used to measure $g-2$ of the electron. This apparatus allows the measurement of the cyclotron frequency ν_c', and the spin-cyclotron-beat (or $g-2$) frequency $\nu_a' = \nu_s - \nu_c'$ on a single electron stored in a Penning trap at $\simeq$4 K. Detection is via Rabi-Landau level-dependent shifts in the continuously monitored axial resonant frequency ν_z induced by a weak magnetic bottle.

This signal is integrated and low-pass filtered to provide a correction voltage which is added to that of the standard cells providing the focusing potential, which determines the axial oscillation frequency [Eq. (2.56)]. The axial oscillation frequency of the electron is thereby locked to the external drive frequency throughout the experiment. Any changes in the "natural" axial oscillation frequency of the electron in the trap are then reflected in changes of the correction voltage needed to maintain ω_z constant. The correction voltage will also monitor long-term voltage drifts of the standard cells, or any battery noise with frequencies less than the inverse of the response time of the feedback loop.

2.4.4 Cyclotron frequency ω_c'

The necessary coupling between the cyclotron or spin motion of the trapped electron and the axial oscillation frequency is provided by an extremely weak magnetic bottle, modifying the uniform magnetic field to one of the form:

$$B_z = B_0 + B_2 z^2.$$

Two such bottles were used, the weaker bottle (B_2 ~120 G/cm^2) was provided by a thin Ni wire wound concentrically around the ring electrode (see Fig. 5), the stronger one (B_2 ~300 G/cm^2) by an iron ring placed outside the vacuum envelope. The coupling provided by these bottles gives a dependence of the axial oscillation frequency on the cyclotron and spin quantum numbers n, m_s:

$$\frac{\delta\omega_z}{2\pi} = \left(n + m_s + \tfrac{1}{2}\right)\delta, \tag{2.62}$$

where $\delta = 1.0$ and 2.5 Hz for the weak and strong bottles, respectively. Thus the "natural" frequency of axial oscillation in the trap depends on the cyclotron and the spin state of the electron. Changes in these states can then be detected, as described above, by the change in the correction voltage generated by the feedback loop to maintain ω_z constant.

The whole apparatus is maintained at a temperature of 4 K. This means that the electron is typically in the lowest four cyclotron levels $0 < n < 4$, in the absence of external perturbation, the average value of n being ~1. The time constant for thermal fluctuations of n is quite short, ~1 sec, compared with that of m_s (spin flips), which is ~several minutes. The quantum transitions of a single electron corresponding to changes in n and m_s can be clearly seen in Fig. 6a, which shows the axial frequency shift ($\propto$ correction voltage) as a function of time for an interval of ~10 min. Spin flips are registered by changes in the "base line" of the much more rapid cyclotron fluctuations. It can be seen from Eq. (2.62) that the minimum values of $\delta\omega_z/2\pi$ are δ, 0 for $m_s = \frac{1}{2}$, $-\frac{1}{2}$, respectively.

The frequency ω_c is now measured by exciting the cyclotron levels by feeding in the RF power of frequency ω_c' (see Fig. 5). Typical cyclotron resonances are shown in Figs. 6b and 6c for the strong and weak magnetic bottles, respectively. The resonance is much narrower for the weak bottle. The side bands at frequencies $\pm\omega_m$, $\pm 2\omega_m$, ... from the shifted cyclotron frequency $\omega_c' = \omega_c - \omega_m$ can be seen. These side bands result from beating between the magnetron and cyclo-

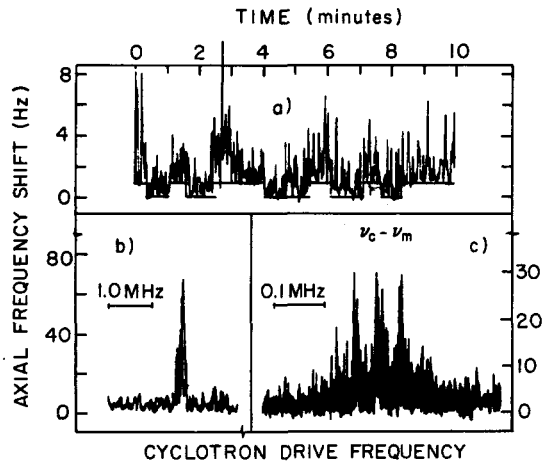

FIG. 6. Observed axial frequency shift $\delta\nu_z = \delta\omega_z/2\pi$ for single trapped electrons in the University of Washington experiment. a) Spin flips are signalled in the 1.0 Hz bottle by ±1.0 Hz changes in the $n = 0$ plateau when ν_a' is applied continuously. The spikes reflect thermal cyclotron excitation. b) Externally excited cyclotron resonances for the 2.5 Hz bottle with a large locking drive. c) The same for the 1.0 Hz bottle with a weak locking drive. For c) $\nu_c - \nu_m = 510\,739\,65$ kHz.

tron motion, and are a consequence of the lack of perfect azimuthal symmetry of the trap, produced by the twisted ends of the Ni wire providing the magnetic bottle.

2.4.5 g - 2 frequency ω_a'

The technique used here is to excite nonresonant axial oscillations at a frequency:

$$\omega_d \approx \omega_z, \quad \omega_d \approx \omega_a' = \omega_L - \omega_c', \tag{2.63}$$

using an auxiliary axial drive circuit (see Fig. 5). In this case the resonance is detected by observing the number of spin flips per unit time, as a function of the auxiliary drive frequency. The spin flips occur as a result of the combined cyclotron and vertical oscillations in the magnetic bottle. Owing to the shape of the magnetic field the electron sees a component transverse both to its velocity and to the main field (B_0). This component changes sign as the electron moves through the plane $z = 0$. In the electron rest frame this field basically rotates at a frequency ω_c' but is modulated in amplitude at the axial drive frequency ω_d. Consequently the electron is in effect subject to the combination of two fields, one rotating at $\omega_c' + \omega_d$ and the other at $\omega_c' - \omega_d$, and spin flips would be induced if either were equal to ω_L'. In the present case the former is applicable and thus the condition given in Eq. (2.63) is met.

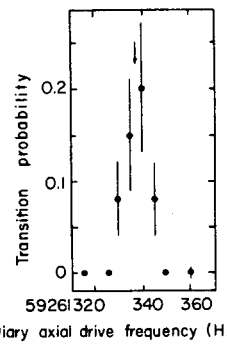

FIG. 7. $g-2$ frequency resonance in the University of Washington experiment. Data are obtained in the $\delta = 1.0$ Hz bottle with alternating detection by counting $n = 0$ plateau changes in ~20 alternating 1 min excitation and detection time intervals. The error bars indicate counting statistics.

In the experiment the electron is locked on to the fixed axial drive at the resonant frequency ω_z which is applied alternately with the auxiliary-off resonance drive near ω_a'. This technique of alternate excitation and detection leads to sharp resonances with respect to the frequency ω_d (see Fig. 7).

2.4.6 Frequency results and a_e

For a sample run the following frequencies were obtained[43]:

$$\left.\begin{aligned} \frac{\omega_c'}{2\pi} &= 51\,072\,915\,(10)\ \text{kHz}, \\ \frac{\omega_z}{2\pi} &= 59\,336\,170.14\,(10)\,\text{Hz}, \\ \frac{\omega_a'}{2\pi} &= 59\,261\,337.5\,(4.5)\,\text{Hz}. \end{aligned}\right\} \tag{2.64}$$

An averaging of the results for eight runs using the shallow magnetic bottle yielded[43]

$$\text{experiment:}\quad a_e = (1\,159\,652\,410 \pm 200)\cdot 10^{-12}, \tag{2.65}$$

which is in excellent agreement with the theoretical prediction for the electron anomaly given by Eq. (2.9):

$$\text{theory:}\quad a_e = (1\,159\,652\,400 \pm 400)\cdot 10^{-12}.$$

2.5 The high-accuracy comparison of the electron and positron magnetic moments at high energy

The present accuracy of the directly measured value of the positron anomaly is only at the level of 0.1% [see Eq. (2.34)] and so comparison with the very precise electron result [Eq. (2.65)] are of limited value. However, a much more accurate comparison is available through the measurements made at high energy in the VEPP-2M storage ring at Novosibirsk by Serednyakov *et al.*[94]

This experiment makes use of the polarization of electrons and positrons under the action of synchrotron radiation and the subsequent resonant depolarization of the beams by the application of an oscillating longitudinal magnetic field. There are aspects of both the precession and the spin resonance techniques involved in this method, as we shall see.

As first pointed out by Ternov, Loskutov and Korovina,[95] the gradual buildup of the polarization perpendicular to both the velocity and the acceleration is due to the emission of spin-flip synchrotron radiation by the ultra-relativistic particles as they are deflected in the magnetic field of the storage ring. In this way, positrons are polarized parallel and electrons antiparallel to the vertical magnetic field. This transverse polarization P builds up according to

$$P = P_0\,(1 - e^{-t/\tau_0}), \tag{2.66}$$

where P_0 is approximately 0.92 and the time constant

τ_0 is given by

$$\tau_0 = \frac{8}{5\sqrt{3}} \frac{m_0^2 c^2 r^3}{e^2 \hbar \gamma^5}, \tag{2.67}$$

with r the radius of curvature of the electron trajectory, which has in effect been assumed to be circular. The experiment was carried out with ~15 mA electron and positron stored currents at an energy of 625 MeV. Under these conditions the time constant for the radiative polarization τ_0 was about one hour.

In the horizontal plane the component of the electron (or positron) spin rotates with the frequency ω_s given by Eq. (2.7):

$$\omega_s = \left(a + \frac{1}{\gamma}\right) \omega_0,$$

where $\omega_0 = e\bar{B}/(m_0 c)$ with $\bar{B}$ the average value of the guiding magnetic field. If we combine this with Eq. (2.28) we can write

$$\omega_s = (1 + \gamma a)\, \omega_c, \tag{2.68}$$

where ω_c, the cyclotron or revolution frequency, is maintained at a fixed value by the external RF generator which keeps the particles on their orbits. Since for the 625 MeV electrons γ has the value ~1200, the product $\gamma a \sim 1.4$ and the spin precesses through about 2.4 turns while the electron passes once around the storage ring. Thus with respect to a fixed point on the electron orbit the spin appears only to have moved through an angle of $0.4 \times 2\pi$ for each revolution of the ring by the particle.

In order to depolarize the ensemble of electrons, the applied longitudinal magnetic field must have a fixed phase relationship with the precessing spin as seen at the particular position of the depolarizer. A frequency ω_r which satisfies this resonance condition is

$$\omega_r = (\gamma a - 1)\, \omega_c. \tag{2.69}$$

In the experiment a longitudinal magnetic field of frequency ω_r was produced by a depolarizing coil placed in one of the straight sections of the storage ring, as shown in Fig. 8.

A special system of counters was placed in another of the straight sections, as is also shown in the figure, and these were used to detect the changes in the polarization of both the electron and the positron beam as the depolarizer frequency was slowly scanned (~5 Hz sec^{-1}) through the region of the resonance condition. The positrons and electrons were distinguished by their arrival time with respect to the phase of the accelerating RF voltage (of frequency ω_c).

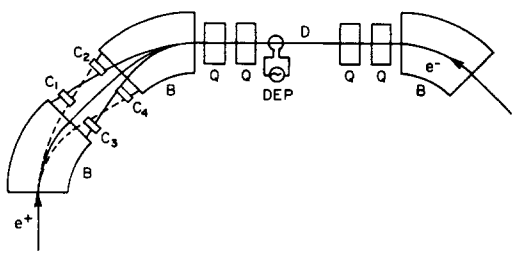

FIG. 8. The apparatus used for simultaneous measurement of e^+, e^- polarization in the storage ring VEPP-2M at Novosibirsk. *B*: bending magnets; *Q*: quadrupole lenses; *DEP*: depolarizer; C_1–C_4: scintillation counters in 4-fold coincidence.

As the electrons circulate the ring, the beam is slowly depleted by elastic electron-electron scattering within the bunches. The elastic cross-section is spin dependent, and consequently this loss mechanism may be used to detect the polarization of the beam.[96] The counters were set to detect pairs of particles between which there had been an energy transfer of 4 to 8%. The beam polarization could contribute up to 10% to the recorded count rate. Thus the passage of the depolarizing frequency through the resonance condition was signalled by a change in the counting rate of this order.

The approximate depolarizing frequency was 7 MHz, and the difference between its precise values for electrons and positrons was found to be less than 250 Hz.

From Eq. (2.69) and using the fact that $\gamma a \sim 1.4$ we can write the experimental result for electrons and positrons with $\gamma \sim 1200$ as[48]

$$\frac{|a_{e^+} - a_{e^-}|}{a_e} < 1.0 \cdot 10^{-5} \tag{2.70}$$

at the 95% confidence level.

At the conclusion of this examination of the measurements of the lepton g-factors we can say that QED has withstood all the challenges of the increasingly accurate experiments. In spite of the fact that the electron g-factor is now measured in two parts in 10^{10}, its value is in complete agreement with the predictions of QED.

For the muon, measurement of the g-factor stands at an accuracy of eight parts in 10^9 and yet no contribution from outside the realm of known interactions is seen, although the effect of strong interactions has been clearly established. No evidence of any extra interaction which might explain the relatively large mass of the muon has been found.

A strength of this situation is that it forms a very good proving ground for theoretical models, in particular of the weak interactions, since their allowed effects on the lepton anomalous magnetic moments are so severely restricted. This applies more specifically to the muon which through its much larger mass is more susceptible to such effects.

3. TESTS OF DISCRETE SYMMETRIES USING FREE DEPTONS

3.1 Tests of CPT

The *CPT* theorem, first noted by Lüders,[97] states that any quantum field theory described by a local Lorentz-invariant Hermitian Hamiltonian is invariant under the combined operations of charge conjugation (*C*), parity (*P*), and time reversal (*T*). The *CPT* transformation is equivalent to strong reflection[98] $X \to -X$ (where X is a four-vector) and Hermitian conjugation. A very clear exposition of the proof of the theorem using this latter approach has been given by Lüders.[99]

A consequence of the theorem is the equality of the masses of particle and antiparticle. Consider a par-

ticle with state vector $\psi = |e, \mathbf{p}, \mathbf{s}\rangle$; $e, \mathbf{p}, \mathbf{s}$ are the charge, momentum, and spin, respectively, of the particle. The *CPT* conjugate state vector $\tilde{\psi}$ is given by

$$\tilde{\psi} = |-e, \mathbf{p}, -\mathbf{s}\rangle.$$

If H is the Hamiltonian describing the free particle, the Schrödinger equation reads:

$$H\psi = E\psi. \tag{3.1}$$

The *CPT* conjugate of Eq. (3.1) is

$$\bar{H}\tilde{\psi} = E\tilde{\psi}, \tag{3.2}$$

which may be written, since $H = \bar{H}$ from the *CPT* theorem,

$$H\tilde{\psi} = E\tilde{\psi}. \tag{3.3}$$

But the eigenvalue E reduces, for $\mathbf{p} = 0$, to the mass of the particle, so in this case Eqs. (3.1) and (3.3) state the the equality of the masses of particle and antiparticle.

The equality of the g-factors of particle and anitparticle may be shown by using Eqs. (3.1) and (3.3), where H now describes not a free particle but one interacting with an external magnetic field **B**. In this case the eigenvalue of Eq. (3.1) takes the form

$$E = m - g\frac{e\hbar}{2mc}\mathbf{sB}. \tag{3.4}$$

The *CPT* conjugate state ($e \to -e$, $\mathbf{s} \to -\mathbf{s}$, $m \to \bar{m}$, $g \to \bar{g}$, $\mathbf{B} \to \mathbf{B}$) will, according to Eq. (3.3), have the same eigenvalue:

$$E = \bar{m} - \bar{g}\frac{e\hbar}{2mc}\mathbf{sB}. \tag{3.5}$$

Since $m = \bar{m}$, it follows from Eqs. (3.4) and (3.5) that:

$$g = \bar{g}.$$

To date, the most accurate test of the equality of the electron and positron magnetic moments was carried out in the VEPP-2M e^+e^- storage ring of Novosibirsk,[94] described in Sec. 2.5. It was found that Eq. (2.70):

$$\frac{|a_{e^+} - a_{e^-}|}{a_e} < 1.0 \cdot 10^{-5} \text{ (95\% confidence level)}$$

or, for the g-factors,

$$\frac{|g_{e^+} - g_{e^-}|}{g_e} < 1.2 \cdot 10^{-8} \text{ (95\% confidence level).}$$

This result is more than two orders of magnitude more precise than that given by combining the best measurements to date of a_{e^+}[79] and a_{e^-}.[92] However, dramatic improvement in the experimental value of a_{e^+} is expected in the near future from the group at the University of Washington, lead by Dehmelt.

The anomalous magnetic moments of both positive and negative muons have been measured with much-increased precision in the recently completed muon storage ring experiment at CERN,[87,88] described in Sec. 2.3 above. The values found are

$$a_{\mu^+} = (1\,165\,912 \pm 11)\cdot 10^{-9},$$
$$a_{\mu^-} = (1\,165\,938 \pm 12)\cdot 10^{-9},$$

giving

$$6 \cdot 10^{-6} > \frac{a_{\mu^+} - a_{\mu^-}}{a_\mu} > -50 \cdot 10^{-6} \text{ (95\% confidence level),}$$

$$7 \cdot 10^{-9} > \frac{g_{\mu^+} - g_{\mu^-}}{g_\mu} > -58 \cdot 10^{-9} \text{ (95\% confidence level).}$$

The best existing upper limits for the fractional difference of the g-factors for positive and negative leptons are therefore of comparable magnitude for electrons and muons, being in both cases $\sim 10^{-7}$.

A further consequence of the *CPT* theorem is the equality of the lifetimes of particle and antiparticle:

$$\tau = \bar{\tau}.$$

This result may readily be derived[100,101] using scattering theory to first order in the Hamiltonian H_{int} of the decay interaction. The result has been proved to hold also for all orders in H_{int} by Lüders and Zumino.[102]

Using the best existing measurements for the μ^+ [103] and μ^- [104] lifetimes at rest,

$$\tau^0_{\mu^+} = 2.19711(8)\ \mu\text{sec}$$

or

$$\tau^0_{\mu^-} = 2.19800(200)\ \mu\text{sec}$$

gives

$$-2.2 \cdot 10^{-3} < \frac{\tau^0_{\mu^+} - \tau^0_{\mu^-}}{\tau^0_\mu} < 1.4 \cdot 10^{-3}$$

(measurements at rest) 95% confidence limits.

The μ^+ and μ^- lifetimes have also been measured in flight at a relativistic γ value of ~29 in the CERN muon storage ring[105] with the results

$$\tau^{\gamma=29}_{\mu^+} = 64.419(58)\ \mu\text{sec}$$
$$\tau^{\gamma=29}_{\mu^-} = 64.368(29)\ \mu\text{sec}.$$

As the Lorentz γ-factor is the same for μ^+ and μ^- to much better than the quoted lifetime errors, it may be concluded from these measurements that

$$-1.4 \cdot 10^{-3} < \frac{\tau^0_{\mu^+} - \tau^0_{\mu^-}}{\tau^0_\mu} < 3.0 \cdot 10^{-3}$$

(measurements in flight $\simeq 29$) 95% confidence limits.

Combining the measurements at rest and in flight for $\tau^0_{\mu^-}$ and using the very precise measurement at rest of $\tau^0_{\mu^+}$ [103] gives the result

$$-4.0 \cdot 10^{-5} < \frac{\tau^0_{\mu^+} - \tau^0_{\mu^-}}{\tau^0_\mu} < 1.6 \cdot 10^{-3}$$

(best average values of $\tau^0_{\mu^+}$, $\tau^0_{\mu^-}$) 95% confidence limits.

3.2 Tests of CP

Given the validity of the *CPT* theorem, then *CP* is either conserved (violated) according to whether time reversal invariance T is conserved (violated). Tests of T alone are described in the following section, but *CP* invariance alone (i.e., independently of *CPT*, T conservation) gives predictions relating particle and antiparticle decays. Consider the matrix element for a particle a at rest, of spin $\mathbf{s}_a$, to decay into a system of particles $b, c, \ldots$ with spins and momenta $\mathbf{s}_b, \mathbf{s}_c, \ldots$; $\mathbf{p}_b, \mathbf{p}_c, \ldots$:

$$M \equiv \langle \mathbf{p}_b, \mathbf{s}_b; \mathbf{p}_c, \mathbf{s}_c, \ldots | H_{\text{int}} | 0, \mathbf{s}_a \rangle. \tag{3.6}$$

Under *CP*

$$\mathbf{s}_a \to \mathbf{s}_{\bar{a}}, \quad \mathbf{p}_a \to -\mathbf{p}_{\bar{a}} \text{ etc.}$$

So if H_{int} is invariant under *CP* Eq. (3.3) gives

$$M = \langle -\mathbf{p}_{\bar{b}},\ s_{\bar{b}};\quad -\mathbf{p}_{\bar{c}},\ s_{\bar{c}};\ \ldots\ |H_{\rm int}|\ 0,\ s_{\bar{a}}\rangle \equiv \overline{M}. \tag{3.7}$$

Taking the modulus squared of Eq. (3.7), this tells us that the rate of decay of a particle into a particular configuration of decay particles is equal to the decay rate of the antiparticle into the same configuration of decay antiparticles with momenta reversed.

Consider muon decay and integrate out the unobserved neutrino variables. The decay electron distribution for positive muons is given by an expression of the form

$$\frac{dn_{e^+}}{dx\, d\cos\theta} = A(x) + B(x)\,\hat{s}_\mu \hat{p}_e, \tag{3.8}$$

where $x = 2p_e/M_\mu$ (p_e = electron momentum in the muon rest frame), and $\cos\theta = \hat{s}_\mu \cdot \hat{p}_e$. Writing a similar expression for μ^- decay,

$$\frac{dn_{e^-}}{dx\, d\cos\theta} = \overline{A}(x) + \overline{B}(x)\,\hat{s}_\mu \hat{p}_e. \tag{3.9}$$

From expressions (3.7), (3.8), and (3.9), it follows that for all electron momenta and angles,

$$A(x) + B(x)\cos\theta = \overline{A}(x) - \overline{B}(x)\cos\theta,$$

so

$$A(x) = \overline{A}(x),\quad B(x) = -\overline{B}(x).$$

This implies that the decay electron asymmetry is equal in magnitude but opposite in sign for μ^+ and μ^- decays. This follows directly from the general CP invariance condition (3.7), independently of the form of A, B (whether the decay is $V-A$, $V+A$, P, S, or T). A direct consequence of this is that the asymmetry observed in the decay electron time spectrum in muon $(g-2)$ experiments (see Sec. 2.2.1) must have the same magnitude for μ^+ and μ^- (provided, of course, the initial degree of polarization of the muons is the same). That this is true in the most recent CERN muon $(g-2)$ experiment[87,88] is indicated in Fig. 9, where the fitted asymmetry for decay electrons above four different energy thresholds is shown as a function of the fraction f of counts above the thresholds, for two μ^+ and four μ^- runs where running conditions were held as stable as possible. The agreement between the μ^+ and μ^- asymmetries can be seen to be well below the 1% level.

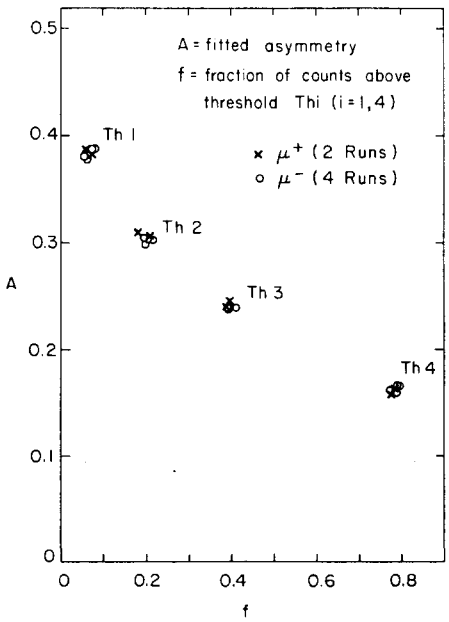

FIG. 9. Fitted asymmetry of the decay electron spectrum in the CERN muon $g-2$ experiment versus counting rate above various electron energy thresholds.

3.3 Tests of T

3.3.1 Time reversal tests in muon decay

In principle it is possible to test T invariance in μ decay, searching for terms in the decay matrix element which are odd under T. For example:

$$s_e\,[s_\mu p_e],$$

i.e., detecting a component of the electron spin transverse to the plane containing the electron momentum and the muon spin. Such experiments are technically very difficult and have so far not been performed. The situation is no easier in radiative muon decay[106] where, as pointed out by Pratt[107] all T-violating terms in the matrix element will either be proportional to transverse (to the electron momentum) components of the electron spin, or to the electron mass. A typical T-violating term of the latter type would be:

$$s_\mu\,[s_e^L k],$$

where $\mathbf{k}$ is the photon momentum and $\mathbf{s}_e^L$ the longitudinal component of the electron spin. The dependence on the electron mass makes such terms significant only for very low electron momenta; so, as in the nonradiative decay, the experimental problems are severe, and no such tests have been performed.

3.3.2 Electric dipole moments

That the existence of an electric dipole moment (EDM) for a free particle is forbidden by parity conservation has been known for some time. However, it was stressed by Purcell and Ramsey[108] that the existence or nonexistence of an EDM for particles should be treated as a purely experimental question, and possible physical mechanisms were suggested that could lead to a nonvanishing EDM. Shortly after the discovery that parity is violated in the weak interactions, it was pointed out by Landau[109] that even if P is violated, the existence of an EDM is still forbidden by T invariance, i.e., the existence of a nonvanishing EDM for some particle implies that both P and T are violated. The validity of the CPT theorem implies, in addition, that CP is also violated. The argument for the vanishing of the EDM for a free particle (in general a state with a well-defined parity) as a consequence of P or T invariance has already been given in Sec. 1 above.

The question of the existence of dipole moments for elementary particles became again of great interest following the discovery of CP[110] (and T)[111] violation in the neutral kaon system. As both T and P had now been shown to be violated in nature, there was now no reason, from discrete symmetries, for the nonexistence of particle EDM's. Estimates of the values to be ex-

pected for the neutron EDM for various *CP* violation models were made by Wolfenstein.[112] With the advent of renormalizable gauge theories of the weak and electromagnetic interactions, it became possible, for the first time, to make reliable calculations[113] of particle EDM's for those theoreis which incorporate *CP* violation in an essential way. A recent example of this type of theory is that proposed by Kobayashi and Maskawa[114] and also studied by Ellis, Gaillard and Nanopoulos,[115] which incorporates six different flavours of quarks. It is generally the neutron EDM [which is currently the most accurately known elementary particle EDM, $D_n = (0.4 \pm 1.1) \times 10^{-24} e$ cm[116]] which is the most sensitive test of such theories, as the *CP* violation is essentially associated with the introduction of heavier quark flavours, which will therefore effect lepton EDM's only through very high order diagrams with large propagator suppression factors. Some predictions[113, 117] however exist for free lepton EDM's in gauge theories, and the present level of experimental sensitivity reached for the electron is already at the level where some theories may be rejected. The best existing measurements for the EDM of the electron and the muon are now described.

3.3.3 Electron EDM measurements

Three types of measurement have been made of the electron EDM: (i) study of the velocity dependence of the precession frequency of the electron spin relative to its momentum vector (i.e., the electron "$g-2$" frequency)[118]; (ii) search for terms in the 180° scattering cross-section of electrons dependent on the electron EDM[119]; (iii) experiments using atomic beams.[120,121]

The technique used in (i) follows from a suggestion originally made by Garwin and Lederman.[122] They pointed out that in $g-2$ precession experiments using magnetic mirror traps (see Sec. 2.2) the electron will experience, in its rest frame, an electric field proportional to the particle velocity as a result of Lorentz transformation of the laboratory magnetic field. This electric field is perpendicular to the magnetic field. If the EDM is nonzero, the spin precession frequency relative to the momentum vector will pick up a component ω_{edm} along the electric field direction in addition to the normal $g-2$ frequency ω_a along the magnetic field direction (Fig. 10). The observed "$g-2$" frequency is then:

$$\omega_a' = \omega_a \left(1 + \frac{f^2}{4a^2}\beta^2\right), \qquad (3.10)$$

where the electric dipole moment is related to f by [see Eq. (1.3)]:

$$D = \frac{f}{2}\frac{e\hbar}{2mc}.$$

Nelson, Schupp, Pidd and Crane[118] searched for a velocity dependence of ω_a' and concluded that

$$D_e \leqslant 3 \cdot 10^{-15}\ e\ \text{cm}.$$

Method (ii) makes use of the high sensitivity of the 180° electron scattering cross-section from a spinless target to terms in the differential cross-section arising from an electron EDM. Rand[119] scattered 100 MeV/c electrons at 180° off a ^{12}C target. A very thorough understanding of systematic errors in the backward differential cross-section (including multiple scattering corrections) is needed in such experiments. It was found that

$$D_e \leqslant 2.3 \cdot 10^{-16}\ e\ \text{cm}.$$

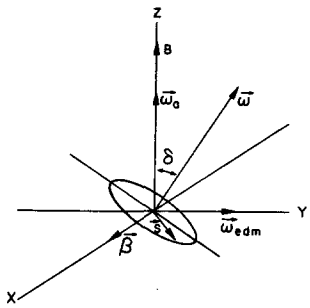

FIG. 10. Angular velocity vector diagram for spin precession in the presence of an EDM. The plane of the precession of the spin $\mathbf{s}$ relative to the velocity $\boldsymbol{\beta}$ is tilted by an angle δ by combining the precession vector due to the anomalous magnetic moment ω_a with that due to the electric dipole moment ω_{edm}.

By far the most precise limits on the electron EDM come, however, from atomic beam resonance experiments using alkali (or alkali-like) atoms. It was first pointed out by Sandars[123, 124] that in such atoms the atomic EDM may be up to ~100 times larger than the intrinsic EDM of the electron. Such effects arise entirely from relativistic parts of the atomic wave function. It had earlier been noted by Schiff[125] that in the nonrelativistic limit the atomic EDM vanishes even if the electron EDM is nonzero. A discussion of the physical basis of the enhancement of the atomic EDM has been given by Ignatovich.[126]

Two experiments of comparable accuracy have been performed. Both search for shifts in the beam resonance frequency[127] on application of an external electric field. The first, that of Weisskopf *et al.*,[120] used beams of Cs and Na atoms. A problem in such experiments is the so-called "$\mathbf{v}\times\mathbf{E}$" effect. The electric field in the laboratory generates a magnetic field in the rest frame of the atom proportional to its velocity. By the Zeeman effect this will lead to a shift of the resonance frequency in the presence of the electric field, and so to a spurious EDM signal. By combining measurements with Cs and Na in the beam, the "$\mathbf{v}\times\mathbf{E}$" contribution was separated from that due to an intrinsic EDM, leading to the result:

$$|D_{Cs}| = (0.8 \pm 1.8) \cdot 10^{-22}\ e\ \text{cm}.$$

The calculations of Sandars indicate that:

$$|D_{Cs}| \approx 119 D_e.$$

So the limit obtained in the electron EDM was [Weisskopf *et al.*[120]]:

$$|D_e| < 3 \cdot 10^{-24}\ e \cdot \text{cm (at 90\% confidence level)}.$$

The second experiment, carried out by Player and Sandars,[121] used an ingenious trick to circumvent the "$\mathbf{v}\times\mathbf{E}$" effect. By choosing an atom of high electric polarizability (they used the excited metastable state $^3P_2$ state of Xe), the quantization axis of the atom is constrained to lie along the electric field direction.

Hence the magnetic field, proportional to $\mathbf{v}\times\mathbf{E}$, is perpendicular to the quantization axis, and at least to first order there is no Zeeman shift. Other residual systematic errors were removed by making a Xe-Kr comparison. (The EDM enhancement factors for Xe, Kr are ~130, 20.) The result found for the electric dipole moment was [Player and Sandars[121]].

$$D_e = (0.7 \pm 1.1)\cdot 10^{-24}\ e\cdot\text{cm (errors at 90\% confidence level)}.$$

The last two measurements of D_e are of comparable accuracy to the best measurement on the free neutron[115] mentioned above.

Note that all these measurements are made on neutral systems. The difficulty of measuring the EDM for charged systems, where any external electric field couples directly to the charge, dominating the interaction energy, was noted by Garwin and Lederman.[122] The best limits for "free" electrons (i) and (ii) above are some 8 or 9 orders of magnitude less precise than the atomic beam measurements.

3.3.4 Muon EDM measurements

One possible way to get a limit on the EDM of the muon is by comparing the experimental[87,88] and theoretical[36] values of the muon anomaly. Attributing the difference in these numbers to a muon EDM effect, and using Eq. (3.10) with $\beta = 1$ ($\gamma = 29.3$ for the muons in the CERN storage ring) leads to[87,88]

$$D_\mu < 8.0\cdot 10^{-19}\ e\cdot\text{cm (95\% confidence limit)}.$$

The muon EDM can, however, be directly measured. Referring to Fig. 10 it can be seen that the precession vector of the spin relative to the momentum is rotated out of the direction of the magnetic field by an angle: $\delta = \omega_{\text{edm}}/\omega_a = f\beta/2a$. As a consequence the decay electrons from the muon will show a time-varying asymmetry along the magnetic field direction. Such an asymmetry was searched for in the first CERN muon $(g-2)$ experiment[82] where muons were brought to rest in a polarimeter. It was concluded that[128]

$$D_\mu = (0.6 \pm 1.1)\cdot 10^{-17}\ e\cdot\text{cm (1 standard deviation error)}.$$

A related technique has been used in the most recent CERN muon storage ring experiment.[129] Looking again at Fig. 10 it is evident that the number of "upward"- and "downward"-going decay electrons (the plane perpendicular to the magnetic field is taken as horizontal) will be modulated at the $(g-2)$ frequency. It is also clear that the modulation will be $\pi/2$ out of phase with that seen in the total "up + down" counting rate, which has maxima or minima when the muon spin vector is either forward- or backward-pointing (see Sec. 2.2.1). As a result the counting rates of "up" and "down" electrons are

$$\begin{aligned} N_{\text{up}} &= \frac{N}{2}\, e^{-t/\tau}\,[1 - A_\mu \cos(\omega t + \varphi) + A_e \sin(\omega t + \varphi)], \\ N_{\text{down}} &= \frac{N}{2}\, e^{-t/\tau}\,[1 - A_\mu \sin(\omega t + \varphi) \mp A_e \sin(\omega t + \varphi)]. \end{aligned} \tag{3.11}$$

A_e is related to the tilt angle δ in Fig. 10, which is in turn related to the muon EDM via the relation

$$\frac{D_\mu}{e} = \frac{a}{2}(\lambda_\mu)\,\delta. \tag{3.12}$$

The relation between δ and A_e may be calculated analytically if all decay electrons with energy $>E_t$ are detected. The result is

$$NA_e = -4\delta\left[\frac{1}{6}\cos^{-1}(a-1) + \sqrt{\frac{2}{a}-1}\left(\frac{a^4}{15} - \frac{7a^3}{45} - \frac{11a^2}{90} + \frac{a}{6}\right)\right], \tag{3.13}$$

where

$$N = 4\pi\left(1 - \frac{5a}{6} + \frac{a^3}{8} - \frac{a^4}{48}\right)$$

and $a = 2E_t/(E_{t_{\max}})$.

The formula (3.13) is exact in the ultra-relativistic limit $p \sim E$ for the decay electron in the muon rest frame. For the energy threshold ~800 MeV used in the CERN experiment, Eq. (3.13) gives $A_e = 0.22\delta$. This sensitivity is somewhat diluted in the actual experiment as the "up" and "down" electrons are tagged, by scintillation counters placed above and below the median plane; so allowing for the finite spread of the stored muons in the vertical direction, not all "up"-going decay electrons are recorded in the "up" scintillator. This leads to a dilution factor of 0.75, or

$$A_e = 0.164\delta. \tag{3.14}$$

The EDM signal is sought by fitting the up and down tagged decay electron time spectra. From Eqs. (3.11) it is evident that if A_e is nonzero there will be a phase difference $\Delta\phi = 2A_e/A_\mu$ between the up and the down time spectra. From the measured phase difference, and A_μ (which is also found from the fit), A_e may be deduced and hence D_μ via Eqs. (3.14) and (3.12).

A full discussion of systematic errors is given in Ref. 129. The errors quoted below are dominantly statistical. Separate measurements were made for μ^+ and μ^- with the results[129]

$$D_{\mu^+} = (8.6 \pm 4.5)\cdot 10^{-19}\ e\cdot\text{cm}, \qquad D_{\mu^-} = (0.8 \pm 4.3)\cdot 10^{-19}\ e\cdot\text{cm}.$$

Assuming opposite EDM's for the particle and antiparticle gives the combined result

$$D_\mu = -(3.7 \pm 3.4)\cdot 10^{-19}\ e\cdot\text{cm}.$$

The sign quoted is for the particle (μ^-). All the errors quoted here are at the one standard deviation level. The result of the experiment may also be expressed in the form

$$|D_\mu| < 1.05\cdot 10^{-18}\ e\ \text{cm (95\% confidence limit)}.$$

This represents an improvement by a factor of 27 over the limit set by the previous experiment.[128] The number is also comparable to the "indirect" estimate of D_μ found by comparing the theoretical and experimental values of a_μ as described above.

ACKNOWLEDGMENTS

The authors would like to thank all members of the muon storage ring collaboration at CERN for many fruitful and enlightening discussions. Special thanks are due to F. J. M. Farley, F. Krienen and F. Lange.

[1]Reviews with special emphasis on electron $(g-2)$ measurements are: A. Rich and J. C. Wesley, Rev. Mod. Phys. 44, 250 (1972). H. D. Dehmelt in Atomic masses and fundamental

constants, 5 (Plenum, New York, 1976), p. 499. The muon $(g-2)$ measurements are described in: J. Bailey and E. Picasso, Progr. Nuclear Phys. 12, 43 (1970). F. Combley and E. Picasso, Phys. Reports 14C, 1 (1974). F. J. M. Farley, Contemp. Phys. 16, 413 (1975). J. H. Field, Proc. EPS Internat. Conf. on High-Energy Physics, Palermo, 1975 (Editrice Compositori, Bologna, 1976), p. 247. A description of the muon $(g-2)$ experiment and an extensive review of the status of QED tests is given in: F. H. Combley, Proc. 7th Internat. Symposium on Lepton and Photon Interactions at High Energies, Stanford University, 1975 (ed. W. T. Kirk) (Stanford, 1975), p. 913.
[2]J. D. Jackson, CERN 77-17 (1977).
[3]P. A. M. Dirac, Proc. Roy. Soc. A 133, 60 (1931); Phys. Rev. 74, 817 (1948).
[4]P. A. M. Dirac, Proc. Roy. Soc. A 117, 610 (1928); A 118, 351 (1928).
[5]P. Kusch, Science 123, 207 (1956); Physics Today 19, 23 (1966).
[6]H. R. Crane, Sci. American 218, 72 (1968); Symposium on High-Energy Physics with Polarized Beams and Targets, Argonne, 1976 (AIP Conf. Proc., USA, No. 35, 1976), p. 306.
[7]J. S. Schwinger, Phys. Rev. 73, 416 (1948); 75, 898 (1949).
[8]P. T. Olsen and E. R. Williams, Proc. 5th Internat. Conf. on Atomic Masses and Fundamental Constants, Paris, 1975 (AMCO-5) (eds. J. H. Sandars and A. H. Wapstra) (Plenum Press, New York, 1976), p. 538.
[9]The fundamental constants are discussed in: E. R. Cohen and B. N. Taylor, J. Phys. Chem. Reference Data 2, 663 (1973). See also the contribution of these authors in AMCO-5, Paris, 1975, p. 663.
[10]H. Suura and E. Wichmann, Phys. Rev. 105, 1930 (1957).
[11]A. Peterman, Phys. Rev. 105, 1931 (1957).
[12]H. H. Elend, Phys. Lett. 20, 682 (1966); 21, 720 (1966).
[13]G. W. Erickson and H. T. Liu, Univ. California, Davis Report UCD-CNL-81 (1968).
[14]R. Karplus and N. M. Kroll, Phys. Rev. 77, 536 (1950).
[15]A. Peterman, Helv. Phys. Acta 30, 407 (1957); Nuclear Phys. 3, 689 (1957).
[16]C. M. Sommerfield, Phys. Rev. 107, 328 (1957).
[17]M. J. Levine, R. C. Perisho and R. Roskies, Phys. Rev. D 13, 997 (1976).
[18]M. J. Levine and R. Roskies, Phys. Rev. D 9, 421 (1974).
[19]R. Barbieri, M. Caffo and E. Remiddi, Phys. Lett. 57B, 460 (1975).
[20]J. A. Mignaco and E. Remiddi, Nuovo Cimento 60A, 519 (1969).
[21]R. Barbieri and E. Remiddi, Phys. Lett. 49B, 468 (1974).
[22]P. Cvitanovic and T. Kinoshita, Phys. Rev. D 10, 4007 (1974).
[23]J. Calmet and A. Peterman, Phys. Lett. 47B, 369 (1973).
[24]J. Aldins, S. J. Brodsky, A. Dufner and T. Kinoshita, Phys. Rev. D 1, 2378 (1970).
[25]C. Chang and M. J. Levine, private communication quoted by the authors of Ref. 17.
[26]M. J. Levine and R. Roskies, Phys. Rev. D 14, 2191 (1976).
[27]M. A. Samuel and C. Chlouber, Phys. Rev. Lett. 36, 442 (1976).
[28]J. Calmet and A. Peterman, Phys. Lett. 58B, 449 (1975).
[29]B. E. Lautrup and M. A. Samuel, Phys. Lett. 72B, 114 (1977).
[30]R. Barbieri and E. Remiddi, Nuclear Phys. B90, 233 (1975).
[31]T. Kinoshita, Nuovo Cimento 51B, 140 (1967).
[32]B. E. Lautrup and E. de Rafael, Phys. Rev. 174, 1835 (1968); Nuovo Cimento 64A, 322 (1964).
[33]B. E. Lautrup, Phys. Lett. 32B, 627 (1970).
[34]B. E. Lautrup, A. Peterman and E. de Rafael, Nuovo Cimento 1A, 238 (1971).
[35]S. J. Brodsky and T. Kinoshita, Phys. Rev. D 3, 356 (1971).
[36]J. Calmet, S. Narison, M. Perrottet and E. de Rafael, Rev. Mod. Phys. 49, 21 (1977).
[37]B. E. Lautrup, Phys. Lett. 38B, 408 (1972).
[38]M. A. Samuel, Phys. Rev. D 9, 2913 (1974).
[39]V. Barger, W. F. Long and M. G. Olsson, Phys. Lett. 60B, 89 (1975).
[40]J. Calmet, S. Narison, M. Perrottet and E. de Rafael, Phys. Lett. 61B, 283 (1976).
[41]M. Gourdin and E. de Rafael, Nuclear Phys. B10, 667 (1969).
[42]A. Bramon, E. Etim and M. Greco, Phys. Lett. 39B, 514 (1972).
[43]R. Jackiw and S. Weinberg, Phys. Rev. D 5, 2396 (1972).
[44]W. A. Bardeen, R. Gastmans and B. E. Lautrup, Nuclear Phys. B46, 319 (1972).
[45]I. Bars and M. Yoshimura, Phys. Rev. D 6, 374 (1972).
[46]K. Fujikawa, B. W. Lee and A. I. Sanda, Phys. Rev. D 6, 2923 (1972).
[47]J. Primack and H. R. Quinn, Phys. Rev. D 6, 3171 (1972).
[48]D. A. Discus, Phys. Rev. D 12, 2176 (1975).
[49]J. P. Leveille, Imperial College London, Preprint ICTP/77-78/2 (1978).
[50]S. J. Brodsky and J. Sullivan, Phys. Rev. 156, 1644 (1967).
[51]T. Burnett and M. Levine, Phys. Lett. 24B, 467 (1967).
[52]B. E. Lautrup, A. Peterman and E. de Rafael, Phys. Reports 3C, 193 (1972).
[53]W. V. Houston, Phys. Rev. 51, 446 (1937).
[54]J. E. Nafe, E. B. Nelson and I. I. Rabi, Phys. Rev. 71, 914 (1947).
[55]G. Breit, Phys. Rev. 72, 984 (1947).
[56]P. Kusch and H. M. Foley, Phys. Rev. 72, 1256 (1947); H. M. Foley and P. Kusch, Phys. Rev. 73, 412 (1948).
[57]P. Kusch and H. M. Foley, Phys. Rev. 74, 250 (1948).
[58]J. H. Gardner and E. M. Purcell, Phys. Rev. 76, 1262 (1949); Phys. Rev. 83, 996 (1951).
[59]S. H. Koenig, A. G. Prodell and P. Kusch, Phys. Rev. 88, 191 (1952).
[60]R. Beringer and M. A. Heald, Phys. Rev. 95, 1474 (1954).
[61]P. A. Franken and S. Liebes Jr., Phys. Rev. 104, 1197 (1956).
[62]I. I. Rabi, Z. Phys. 49, 507 (1928).
[63]See, for example, W. K. Louisell, Quantum statistical properties of radiation (Wiley, New York, 1973), p. 318 *et seq.*
[64]F. Bloch, Physica 19, 821 (1953).
[65]H. A. Tolhoek and S. R. DeGroot, Physica 17 (1951).
[66]N. F. Mott, Proc. Roy. Soc. A 124, 425 (1929).
[67]H. Dehmelt, Phys. Rev. 109, 381 (1958).
[68]F. M. Penning, Physica 4, 71 (1937).
[69]T. R. Pierce, Theory and design of electron beams (Van Nostrand, Princeton, New Jersey, 1949).
[70]H. Dehmelt, Spin resonance of free electrons, Report NSF-G5955, 1961.
[71]G. Gräff, F. G. Major, R. W. H. Roeder and G. Werth, Phys. Rev. Lett. 21, 340 (1968).
[72]G. Gräff, E. Klempt and G. Werth, Z. Phys. 222, 201 (1969).
[73]D. Wineland, P. Ekstrom and H. Dehmelt, Phys. Rev. Lett. 31, 1279 (1973).
[74]W. H. Louisell, R. W. Pidd and H. R. Crane, Phys. Rev. 94, 7 (1954).
[75]A. A. Schupp, R. W. Pidd and H. R. Crane, Phys. Rev. 121, 1 (1961).
[76]J. C. Wesley and A. Rich, Phys. Rev. A 4, 1341 (1971).
[77]S. Granger and G. W. Ford, Phys. Rev. Lett. 28, 1479 (1972).
[78]M. Deutsch, Phys. Rev. 82, 455 (1951).
[79]J. Gilleland and A. Rich, Phys. Rev. A 5, 38 (1972).
[80]G. W. Ford, J. L. Luxon, A. Rich, J. C. Wesley and V. L. Telegdi, Phys. Rev. Lett. 29, 1691 (1972). This method was first proposed by V. L. Telegdi, see: L. Grodzins, Progr. Nuclear Phys. 7, 219 (1959).
[81]D. Newman, E. Swetman and A. Rich, in AMCO-5, Paris 1975, p. 506.
[82]G. Charpak, F. J. M. Farley, R. L. Garwin, T. Muller, J. C. Sens, V. L. Telegdi and A. Zichichi, Phys. Rev. Lett. 6, 128 (1961). G. Charpak, F. J. M. Farley, R. L. Garwin, T. Mul-

ler, J. C. Sens and A. Zichichi, Nuovo Cimento 37, 1241 (1965).
[83]D. P. Hutchinson, J. Menes, G. Shapiro and A. M. Patlach, Phys. Rev. 131, 1351 (1963). For a review of early work on the muon g-factor, see: F. J. M. Farley, Progr. Nuclear Phys. 9, 257 (1964), where references to previous experiments are given.
[84]J. F. Lathrop, R. A. Lundy, V. L. Telegdi, R. Winston and D. D. Yovanovitch, Nuovo Cimento 17, 109 (1960). J. F. Lathrop, R. A. Lundy, S. Penman, V. L. Telegdi, R. Winston and D. D. Yovanovitch, Nuovo Cimento 17, 114 (1960).
[85]S. Devons, G. Gidal, L. M. Lederman and G. Shapiro, Phys. Rev. Lett. 5, 330 (1960).
[86]J. Bailey, W. Bartl, G. von Bochmann, R. C. A. Brown, F. J. M. Farley, M. Giesch, H. Jöstlein, S. Van der Meer, E. Picasso and R. W. Williams, Nuovo Cimento A9, 369 (1972).
[87]J. Bailey, K. Borer, F. Combley, H. Drumm, C. Eck, F. J. M. Farley, J. H. Field, W. Flegel, P. M. Hattersley, F. Krienen, F. Lange, G. Petrucci, E. Picasso, H. I. Pizer, O. Rúnolfsson, R. W. Williams and S. Wojcicki, Phys. Lett. B55, 420 (1975). J. Bailey, K. Borer, F. Combley, H. Drumm, F. J. M. Farley, J. H. Field, W. Flegel, P. M. Hattersley, F. Krienen, F. Lange, E. Picasso and W. von Rüden, Phys. Lett. 67B, 225 (1977).
[88]J. Bailey *et al.*, to be published.
[89]K. M. Crowe, J. F. Hague, J. E. Rothberg, A. Schenck, D. L. Williams, R. W. Williams and K. K. Young, Phys. Rev. D 5, 2145 (1972).
[90]D. E. Casperson, T. W. Crane, A. B. Denison, P. O. Egan, V. W. Hughes, F. G. Mariam, H. Orth, H. W. Reist, P. A. Souder, R. D. Stambaugh, P. A. Thompson and G. zu Putlitz, Phys. Rev. Lett. 38, 956 (1977).
[91]R. Van Dyck Jr., P. Ekström and H. Dehmelt, Nature 262, 776 (1976).
[92]R. S. Van Dyck Jr., P. B. Schwinberg and H. Dehmelt, Phys. Rev. Lett. 38, 310 (1977).
[93]A. A. Sokolov and Yu. G. Pavlenko, Optics and Spectrosc. 22, 1 (1967).
[94]S. I. Serednyakov, V. A. Sidorov, A. N. Skrinsky, G. M. Tumaikin and Iu. M. Shatunov, Phys. Lett. 66B, 102 (1977).
[95]I. M. Ternov, Yu. M. Loskutov and K. L. Korovina, Zh. Esper. Teor. Fiz. 41, 1294 (1962).
[96]V. N. Baier and V. A. Khoze, Atomnaya Energiya 25, 440 (1968). V. N. Baier, Uspekhi Fiz. Nauk 105, 441 (1971).
[97]G. Lüders, K. Danske, Vidensk. Selsk. Mat. -Fys. Medd. 28, No. 5 (1954).
[98]W. Pauli in Niels Bohr and the development of physics (Pergamon Press, London, 1955), p. 30.
[99]G. Lüders, Ann. Phys. (USA) 2, 1 (1957).
[100]K. Nishijima, Fundamental particles (Benjamin, New York, 1963), p. 335.
[101]S. Gasiorowicz, Elementary particle physics (Wiley, New York, 1966), p. 513.
[102]G. Lüders and B. Zumino, Phys. Rev. 106, 345 (1957).
[103]M. P. Balandin, V. M. Crebenyuk, V. G. Zinov, A. D. Konin and A. N. Ponomarev, Soviet Phys. JETP 40, 811 (1974).
[104]S. L. Meyer, E. W. Anderson, E. Bleser, L. M. Lederman, J. L. Rosen, J. Rothberg and I. T. Wang, Phys. Rev. 132, 2693 (1963).
[105]J. Bailey, K. Borer, F. Combley, H. Drumm, F. J. M. Farley, J. H. Field, W. Flegel, P. M. Hattersley, F. Krienen, F. Lange, E. Picasso and W. von Rüden, Nature 268, 301 (1977).
[106]C. Fronsdal and H. Überall, Phys. Rev. 113, 654 (1959).
[107]R. H. Pratt, Phys. Rev. 111, 649 (1958).
[108]E. M. Purcell and N. F. Ramsey, Phys. Rev. 78, 807 (1950).
[109]L. D. Landau, Nuclear Phys. 3, 127 (1957).
[110]J. H. Christenson, J. W. Cronin, V. L. Fitch and R. Turlay, Phys. Rev. Lett. 13, 138 (1964).
[111]K. R. Schubert, B. Wolff, J. C. Chollet, J. M. Gaillard, M. R. Jane, T. J. Ratcliffe and J. P. Repellin, Phys. Lett. 31B, 662 (1970).
[112]L. Wolfenstein, Nuclear Phys. B77, 375 (1974).
[113]A. Pais and J. R. Primack, Phys. Rev. D 8, 3036 (1973).
[114]M. Kobayashi and K. Maskawa, Progr. Theor. Phys. 49, 652 (1973).
[115]J. Ellis, M. K. Gaillard and D. V. Nanopoulos, Nuclear Phys. B109, 213 (1976).
[116]W. B. Dress, P. D. Miller, J. M. Pendlebury, P. Perrin and N. F. Ramsey, Phys. Rev. D 15, 9 (1977).
[117]T. D. Lee, Phys. Rev. D 8, 1226 (1973).
[118]D. F. Nelson, A. A. Schupp, R. W. Pidd and H. R. Crane, Phys. Rev. Lett. 2, 492 (1959).
[119]R. E. Rand, Phys. Rev. B 140, 1605 (1965).
[120]M. C. Weisskopf, J. P. Carrico, H. Gould, E. Lipworth and T. S. Stein, Phys. Rev. Lett. 21, 1645 (1968).
[121]M. A. Player and P. G. H. Sandars, J. Phys. B3, 1620 (1970).
[122]R. L. Garwin and L. M. Lederman, Nuovo Cimento 11, 776 (1959).
[123]P. G. H. Sandars, Phys. Lett. 14, 194 (1965).
[124]P. G. H. Sandars, Phys. Lett. 22, 290 (1966).
[125]L. I. Shiff, Phys. Rev. 132, 2580 (1963).
[126]V. K. Ignatovich, Soviet Phys. JETP 29, 1084 (1969).
[127]N. F. Ramsey, Phys. Rev. 76, 996 (1949).
[128]G. Charpak, F. J. M. Farley, R. L. Garwin, T. Muller, J. C. Sens and A. Zichichi, Nuovo Cimento 22, 1044 (1961).
[129]J. Bailey, K. Borer, F. Combley, H. Drumm, F. J. M. Farley, J. H. Field, W. Flegel, P. M. Hattersley, F. Krienen, F. Lange, E. Picasso and W. von Rüden, New limits on the electric dipole moment of positive and negative muons, to be published in Journal of Physics G (Nuclear Physics).